A Multidisciplinary Airplane Research Integrated Library With Applications To Partial Turboelectric Propulsion

Thierry Druot, Mathieu Belleville, Pascal Roches, François Gallard, Nicolas Peteilh, Anne Gazaix

A Multidisciplinary Airplane Research Integrated Library With Applications To Partial Turboelectric Propulsion

T. Druot*
Ecole Nationale de l'Aviation Civile, Toulouse, France
Airbus Operations SAS, Toulouse, France

M. Belleville†
Airbus Operations SAS, Toulouse, France

P. Roches‡
Ecole Nationale de l'Aviation Civile, Toulouse, France

F. Gallard§
Institute of Technology IRT Saint Exupéry, Toulouse, France

N. Peteilh¶
Ecole Nationale de l'Aviation Civile, Toulouse, France

A. Gazaix‖
Institute of Technology IRT Saint Exupéry, Toulouse, France

The aim of this paper is to present a new model library developped as a new test case to benchmark optimization algorithms and Multidisciplinary Design Optimization (MDO) formulations. It introduces the MARILib software (Multidisciplinary Airplane Research Integrated Library). MARILib's first objective is to provide models for research on a wide range of aircraft concepts, from business jets to super jumbos, and also some unconventional configurations, through an Overall Aircraft Design (OAD) approach. The second objective is to share a new benchmark test case for MDO strategies, which does not raise intellectual property issues. The third objective is to describe a case study for educational and training purposes. MARILib will be available as Open Source.

1. Nomenclature

Without special notice, all units are international standard units.

$(.)_{fan}$	=	quantity related to the fan
$(.)_{Free\ Stream}$	=	quantity related to free stream
$(.)_{hybrid}$	=	quantity related to the hybrid architecture
$(.)_{Inlet}$	=	quantity related to the inlet
$(.)_{jet}$	=	quantity related to the jet
$(.)_0$	=	quantity related to reference turbofan without hybridation
δ_0	=	theoretical boundary layer thickness around a cylindrical fuselage of length L
δ_1	=	assessed boundary layer thickness around the e-fan hub
δ	=	boundary layer thickness
η_{eF}	=	"propeller like" e-fan efficiency
η_C	=	wire conductivity efficiency

*Associate Professor, Air Transport department, thierry.druot-ext@enac.fr
†Expert Engineer, Future Project Office, mathieu.belleville@airbus.com
‡Associate Professor, Air Transport department, pascal.roches@enac.fr
§Research Engineer, System Engineering and Modeling department, francois.gallard@irt-saintexupery.com
¶Associate Professor, Air Transport department, nicolas.peteilh@enac.fr
‖MDO team leader, Systems Engineering and Modeling Department, on leave from Airbus Operations SAS, Toulouse, France

η_E	=	global efficiency of the electric chain
η_F	=	"propeller like" fan efficiency
η_G	=	electrical generator efficiency
η_H	=	global factor on fuel efficiency due to hybridation
η_M	=	electric motor efficiency
η_W	=	power electronics efficiency
η_x	=	fan efficiency
γ	=	heat capacity ratio of the air
ρ_0	=	air density at zero altitude in standard atmosphere
ρ	=	air density
A_{Fan}	=	area of the e-fan
A_{Nozzle}	=	nozzle area
Cd_{Cone}	=	clean fuselage tail cone drag coefficient
$Cd_{Cone\ BLI}$	=	tail cone drag coefficient after rear fan installation
Cp	=	specific heat capacity at constant pressure of the air: $1004.5J/kg/K$
D_f	=	diameter of the fuselage
D_{Fan}	=	diameter of the e-fan
D_h	=	diameter of the hub of the electric nacelle
$D_{Nacelle}$	=	diameter of the electric nacelle
D_{Nozzle}	=	diameter of the nozzle of the electrical nacelle
D_0	=	nacelle diameter of the reference turbofan without hybridation
D_1	=	nacelle diameter of the turbofan with hybridation
F_{Core}	=	thrust delivered by the engine core
F_{eFan}	=	thrust delivered by the electric fan
F_{Fan}	=	thrust delivered by the engine fan
Fn_0	=	total thrust of the reference turbofan without hybridation
Fn_1	=	total thrust of the turbofan with hybridation
Fn	=	total thrust
K_a	=	proportion of the remaining tail cone wetted area after rear fan installation
K_{BLI}	=	factor on e-fan thrust to account for boundary layer ingestion
K_{Fn}	=	hybridation thrust ratio of the turbofan
K_C	=	core thrust ratio
K_D	=	engine core diameter ratio
K_M	=	engine core mass ratio
K_W	=	hybrid power ratio
kFn_1	=	rating related thrust factor
kFn_2	=	mach and by-pass-ratio thrust factor
L_{ft}	=	length of the fuselage tail cone
$L_{Nacelle}$	=	length of the e-fan duct
L	=	distance from which the boundary layer develops
m_{Fuel}	=	fuel mass
M_{TF}	=	basic installed turbofan mass
M_{TF0}	=	basic installed mass of the reference turbofan without hybridation
M_{TF1}	=	basic installed mass of a pure turbofan having the same reference thrust than the turbofan with hybridation
M_{TF2}	=	corrected installed mass of the turbofan with hybridation to account for the unchanged core
$Mach_{BL}(y)$	=	mean Mach in a ring of height y above the surface of the hub
$Mach$	=	cruise Mach number
P_{amb}	=	ambiant pressure
P_{stag}	=	stagnation pressure (i.e. total pressure)
P_{stat}	=	static pressure
$Q_{BL}(y)$	=	air flow captured in a ring of height y above the surface of the hub
Q	=	air flow going through the e-fan
R	=	ideal gaz constant for the air
Re	=	Reynolds number

SFC_0	=	specific fuel consumption of the reference turbofan without hybridation
SFC_H	=	specific fuel consumption of the hybrid propulsion system
T_{amb}	=	ambiant temperature
T_{stag}	=	stagnation temperature (i.e. total temperature)
T_{stat}	=	static temperature
V_{Air}	=	free stream air velocity
$V_{BL}(y)$	=	mean air velocity in a ring of height y above the surface of the hub
V_{in}	=	e-fan inlet air velocity
V_{jet}	=	jet velocity
V_{snd}	=	sound velocity at cruise altitude
v	=	local mean air velocity above the surface
W_{eShaft}	=	shaft power delivered to the electrical fan
W_{S1}	=	shaft power delivered to the fan of the turbomachine
W_{S2}	=	shaft power delivered to the electric generator
W_{Shaft}	=	shaft power
y	=	height above the surface

2. Introduction

Researchers developing optimization algorithms use benchmark analytic optimization problems such as the Rosenbrock function, or the CUTEr [1] and CUTEst [2] test suites to assess the relative performance of algorithms. These hundreds of benchmark problems are recognized by the research community, as these papers were cited more than 700 times.

MDO brings new challenges for benchmarking algorithms compared to standard optimization, because of the deeply structured nature of MDO problems. In MDO, a complex system is decomposed into multiple disciplines, each discipline depends on variables that may be shared with other disciplines, or that may be computed by one of them (so called the coupling variables). The MDO algorithms must take that structure into account to appropriately and efficiently solve the MDO problems. The resolution processes are then organized according to different strategies, and there exist multiple ways of creating optimization problems from such processes. The combination of the two defines the MDO architecture, or MDO formulations [3]. There currently exists a set of benchmark problems in MDO, among which the Sellar, Propane combustion, Sobjeski's SSBJ [4] problems. Those problems are used by the MDO community, but they are either unrelated to aircraft design, or, for the SSBJ test case, do not rely on physical equations, since the discipline's outputs are mostly based on arbitrary interpolation coefficients. This is an issue because the mathematical properties of the models (continuity, differentiability, monotony, multi-modality) have a large effect on the relative performance of the algorithms. On the other hand, there exists open source conceptual design libraries such as SUAVE [5], but the problem is not decomposed into disciplines directly interfaced with MDO frameworks, although it was partially interfaced for the mission time integration [6].

Therefore, we identified six main issues that must be addressed towards building an equivalent to CUTEst for the MDO community:

- Issue 1: The purpose of MDO algorithms (or MDO formulations) is to exploit the problem structure, so these problems must be structured
- Issue 2: The problem structure of benchmarks must be representative of real MDO problems, such as aircraft design
- Issue 3: the problem's equations must be based on physical equations with known assumptions, or reproducible statistical regressions on known data or models.
- Issue 4: the problems must be fast to execute, to enable benchmarks
- Issue 5: the problems' definition must be shared
- Issue 6: the benchmarks must be numerous to avoid over tuning of algorithms on a problem dependent feature

MARILib aims to contribute to address the five first issues, and partially the last one, by providing a set of MDO problems along with MARILib.

MARILib contains models that not only address a single airplane concept, but a range of concepts from business jets to super jumbos, and also some unconventional configurations. Indeed, in many research studies initiated in cooperation between Industries and Research Laboratories, it appeared to be difficult to find as starting point a reference airplane description which would be globally consistent, which would correspond to a given set of Top Level Requirements, and which does not raise intellectual property issues. As of today, the development status of MARILib enables to:

1) Generate test cases for MDO experimentation: about 100 functions representing about one thousand lines of codes covering all disciplines: Geometry, Mass and Center of Gravity CG, Propulsion, Aerodynamics, Mission, Low speed and High speed performances, Handling Quality (tail sizing), Costs, Environment and basic design processes.
2) Build a consistent description of a twin turbofan engine airplane designed from only 3 requirements:
   - Passenger capacity (from about 8 to 600 passengers)
   - Nominal range (from about 2000NM to 8000NM)
   - Cruise Mach number (from about 0.5 to 0.85)
3) Integrate a simple modelling of hybrid propulsive architecture (Starc ABL like) and deliver consistent results when comparing hybrid to classical arrangement.

The paper is divided into four parts. A first section presents the overall characteristics of the physical description of the airplane in MARILib, the physical principles applied to implement the design capability and a kind of design process classically used in conceptual design. The second section presents how the model can take into account a hybrid architecture similar to the NASA Starc ABL. The third section presents some results that were obtained when applying a design process to this hybrid configuration. Finally, the fourth section presents how to integrate MARILib into the Generic Engine for MDO Scenarios (GEMS).

3. Model characteristics

A. Library overview

Presently, the model is only capable to model tube and wing airplanes with two or four turbofan engines. It is split into 12 components, including the aircraft itself, each of them described by specific variables, as shown on Table 1.

As a result of this, 160 variables describe the whole aircraft, 120 additional variables, not mentioned in the above table, quantify most important operational performances of the aircraft, which brings to 280 the total number of variables of the whole model for a twin turbofan tube and wing. The list of variables and their signification is given in appendix.

MARILib has been initially programmed in Scilab and then have been migrated to Python. All formulas in the code takes and delivers values in international standard units (m, kg, s, J, N, W, . . .). No formula presented in this paper will be associated with specific units, standards units are assumed everywhere (ranges are in meter, specific fuel consumptions are in kg/N/s, . . .).

At this stage of the migration to Python language, initial Scilab functions have not yet been distributed into object methods, more experience on the library is required to define the best contour of the future objects.

The top level folder architecture is presented in Fig. 1.

The organization of the present implementation of the airplane model is based on a split between attributes related to the aircraft taken as a whole (aircraft level) and attributes related to airplane components. Three main folders are packaging the aircraft model, the two first ones (**aircraft_data** and **aircraft model**) defines aircraft level attributes, the third one (**airplane**) defines component level attributes:

- **aircraft_data**: defines the *Aircraft* class which stores all the characteristics of a given airplane design along the progression of the design process. In addition, there are two Python files defining respectively:
  - Physical performances at airplane level (Aerodynamics, Propulsion, Weights and CGs)
  - Operational performances (Low speeds, High Speeds, Missions, Economics and Environment)

- **aircraft model**: defines functions that applies at aircraft level. These functions are split into the following two sub-folders:
  - **airplane** contains four files with functions related to: aerodynamics, airplane design, regulation, and visualization.

Table 1 Number of descriptive variables of the airplane model in MARILib

Component	Geometry	Mass & CG	Other
Cabin	7	4	
Payload		10	
Tank	9	2	
Landing gear		2	
Fuselage	5	2	
Wing	29	2	
Horizontal tail	19	2	1
Vertical tail	18	2	
Pylon		2	
Nacelle	14	2	4
Engine	3		5
Aircraft		16	
Total	104	46	10

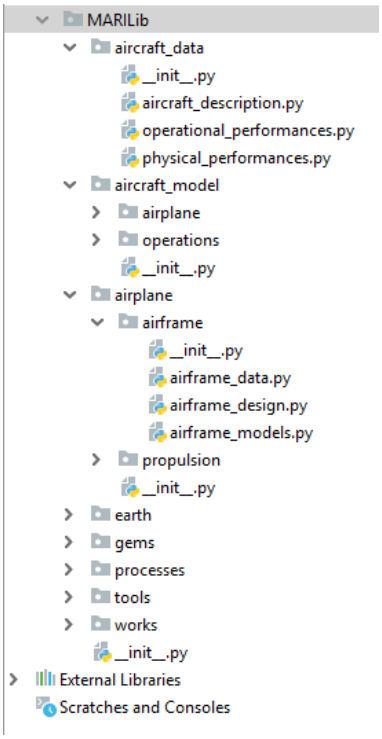

Fig. 1 MARILib top level folder architecture

  - **operations** contains five files with functions related to: environmental impact, flight mechanics, handling qualities, mission, princing and costing.

- **airplane**: is dedicated to component classes and functions. It is split into two sub-folders, one dedicated to airframe components and the other to propulsion components.

  The **airframe** sub-folder contains three Python files:
  - *airframe_data* defines the component classes (cabin, fuselage, wing, . . .)

- *airframe_design* defines the functions which are used to predesign components attributes before any process has been applied or during design processes. The variables that will be defined by running the design process must be instantiated with initial values to run these functions.
- *airframe_models* defines the component related functions which are necessary to simulate aircraft operations. These functions are mainly related to local aerodynamic coefficients.

The **propulsion** sub-folder reproduces this three-file architecture for propulsion system and contains presentely only two different systems : *turbofan* and *hybrid partial turboelectric n1*. Each of these systems is described using three files as explained above (*xyz* stands for the type of propulsion system) :

- *xyz_data* for classes definition,
- *xyz_design* for predesign functions, and
- *xyz_models* for simulations.

Two additional small libraries are completing the aircraft model:

- **earth** contains a model of standard atmosphere as well as some complementary data about earth environment and fuel characteristics
- **tools** provides some math functions and a small unit conversion library.

Finally, the folder **processes** contains process bricks for design. One of the most important file is **initialization** which contains all functions providing default values for design. These default values are parameterized by only five parameters:

- design_range: the nominal range used to size the aircraft,
- cruise_mach: the nominal Mach number of the aircraft during cruise,
- n_pax_ref: the nominal number of passengers used to size the cabin, generally, it is a two-class layout,
- propu_config: the propulsive architecture (1 : for turbofan, 2 : for partial turboelectric),
- n_engine: the number of engines which is basically 2 (4 is accepted but not fully tested at that time).

More details are given in the next section about initialization.

A typical design sequence can be assemble using functions provided in the library processes. Here below, is presented a sequence composed with highly integrated blocks:

```
# Initialization
#=========================================================================
propulsive_architecture = 1 # 1:turbofan, 2:partial turboelectric

# Creation of an instance of the Aircraft objet
aircraft = Aircraft(propulsive_architecture)
n_pax_ref = 150
design_range = unit.m_NM(3000)
cruise_mach = 0.78
number_of_engine = 2
run.aircraft_initialize(aircraft,
                        n_pax_ref,
                        design_range,
                        cruise_mach,
                        propulsive_architecture,
                        number_of_engine)

# Modify initial values here if required
#=========================================================================
aircraft.turbofan_engine.reference_thrust = 130000.
aircraft.wing.area = 149

# Sequencial process
#=========================================================================

# Solve the geometric coupling between airframe and engines
run.aircraft_pre_design(aircraft)

# Solve mass coupling between design and component masses
run.mass_mission_adaptation(aircraft)
```

```
# Perform handling quality analysis
run.eval_handling_qualities_analysis(aircraft)

# Calculate all airplane performances including economics
run.eval_performance_analysis(aircraft)
```

At the end of this process, all required quantities are available to be able to loop the sequence within an optimization process. Next section will present the underlying methodology which is classical.

B. Design principles

The design process is posed as an inverse problem: the main performance features of the aircraft are known and the computational procedure aims at finding its detailed definition to match these performances. In the context of airplane design this question is treated as an optimization problem which aims to define the top level parameters of an airplane which would minimize (or maximize) a given criterion whilst ensuring a given set of constraints.

The cost function and constraints must have design parameters (WingArea, EngineSize, . . .) as input, which requires the existence of a parametric model of the airplane.

$$\begin{aligned} \min_{X=(WingArea,EngineSize,MTOM)} \quad & Criterion(X)(e.g.Cost) \\ \text{s.t.} \quad & g_i(X) \leq {g_i}^{constr} \qquad \forall i \in [1,n] \end{aligned} \tag{1}$$

The target performances are expressed in term of:
1) Mission Requirements (range, speed, seat capacity, . . .)
2) Operational constraints (take off field length, approach speed, time to climb, ceilings, . . .)
3) Customer-Oriented performance criteria (fuel, weight, cost, present value, . . .)

The physical parameters defining the aircraft are split into:
1) Design variables (wing area, span, engine max thrust, empennage areas, . . .)
2) Technological assumptions (materials, engine type, actuator type, regulation, . . .)

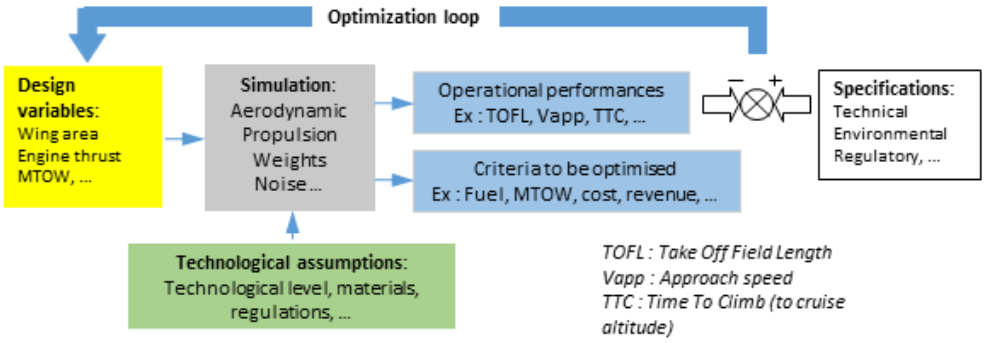

Fig. 2 Optimization loop

The core process of the aircraft conceptual design follows the steps:
1) Expression of Top Level Requirements (TLRs), most important ones are Nominal number of passengers, design range and cruise Mach number.
2) Expression of design assumptions, ex: overall topology, number of front seats, number of aisles, number of engines, empennage type (classical or T-tail), . . . These design assumptions may evolve in the future but a starting values are needed to be able to run the models.
3) Initialization of design variables. This can be done by taking values from an existing aircraft close to the targetted one in term of TLRs or by considering the top level categories which are determined by nominal number of

passengers, design range and cruise Mach number. This last approach is used in the initialization functions. At this stage, we suppose that a model chain exists that can produce all required quantities of interest.

4) Application of a design process (e.g. Multi Discipline Feasible (MDF)) to converge the aircraft definition towards a solution.
5) Processing of sensitivity studies to understand the rational of the exhibited solution.

Steps 4 and 5 may trigger several loops restarting at any previous steps of the process as long as a consistent set of TLRs and design assumptions is not reached according to engineering judgment and client wishes. An overall representation of the core process is shown in Fig. 2.

The proposed library can manage automatically the process from step 1 to step 4, of course by taking some strong assumptions about TLRs. Step 5 is handled by the MDO library GEMS [7],[8], which usage along with MARILib is briefly introduced in the present paper.

A minimal amount of information is required to initialize the process :

- **propu_config** : the propulsive architecture (1 : for turbofan, 2 : for partial turboelectric),
- **n_engine** : the number of engines which is basically 2 (4 is accepted but not fully tested at that time).
- **design_range** : the nominal range used to size the overall aircraft,
- **cruise_mach** : the nominal Mach number of the aircraft during cruise,
- **n_pax_ref** : the nominal number of passengers used to size the aircraft, generally, it is a 2 class layout, sometimes 3 class for long range.

Initialization functions will provide all complementary data to initiate the first run of the model chain. For instance, the choice between under wing engine mounting or rear fuselage mounting will be done according to the required number of passengers. Of course, one can overwrite initialization values with his own ones.

All initializations are implemented in the function *aircraft_initialize(. . .)* in the *processes.design* library. This function must be called before any design activity, but it is possible to overwrite any initialized variable afterward. Among all initialization, most important ones are probably those related to the Top Level Requirements (TLRs) listed below :

- **n_pax_front**: number of seats in a row (economic class),
- **n_aisle**: number of aisle (economic class),
- **m_pax_nominal**: nominal mass allowance for one passenger (passenger + luggage),
- **m_pax_max**: maximum mass allowance for one passenger (passenger + luggage),
- **ref_cruise_altp**: reference cruise altitude (most often used altitude for cruise),
- **top_of_climb_altp**: required top of climb (may be lower than reference cruise altitude),
- **req_oei_altp**: required one engine ceiling altitude,
- **nacelle_attachment**: 0: under wing, 1: rear fuselage,
- **reference_thrust**: generally sea level static thrust (the driving parameter of engine size, weight, consumption and thrust),
- **bpr**: by pass ratio of installed turbofans,
- **wing_area**: wing reference area,
- **wing_aspect_ratio**: wing aspect ratio,
- **hld_type**: type of high lift devices (0 to 10: from clean wing to various combinations of slats and flaps),
- **htp_attachment**: type of empennages, 0: classical, 1: T-tail,
- **range_cost_mission**: range of the cost evaluation mission,
- **utilization**: number of airplane rotation per year,
- **req_tofl**: maximum take-off field length at Maximum Take Off Weight (MTOW) and given conditions,
- **req_app_speed**: maximum approach speed at Maximum Landing Weight (MLW) and given conditions,
- **req_ttc**: maximum Time To Climb to top_of_climb_altp,
- **req_oei_slope**: minimum air path for one engine ceiling estimation,
- **req_vz_climb**: minimum climb speed at 97%MTOW, nominal initial cruise altitude and Max CLimb (MCL) rating,
- **req_vz_cruise**: minimum climb speed at 97%MTOW, nominal initial cruise altitude and Max CRuise (MCR)

rating,

Once initialization is completed, the design activity can start. The sizing of airplanes components are ensured by a set of functions called *eval_component_name_design(. . .)* and *eval_component_name_mass(. . .)*. These functions are based on very simple formulas. The formula's complexity is a trade between accuracy and computational time. Most of them are linear regressions. Public data were used when available or simplifications of known formulas coming from [9–16] were made. The underlying idea is not to be accurate in value prediction but to give robust orders of magnitude through the full design domain going from business jets to super jumbos. Moreover, when some quantities do not vary a lot across the domain, they have been taken as constants. If one knows better formulas in a specific context, it is easy to replace provided ones and take benefit of the overall model integration of MARILib.

Examples of formula for geometrical predesign:

$$cabin\_width = 0.15 + 0.38\, n\_pax\_front + 1.05\, n\_aisle \tag{2}$$

$$fuselage\_width = cabin\_width + 0.40 \tag{3}$$

$$vtp\_aspect\_ratio = 1.7 \tag{4}$$

$$htp\_aspect\_ratio = 5 \tag{5}$$

Concerning mass estimation functions, the rationale is that matter is roughly distributed on surfaces, so, all structural mass estimation functions are based on a given weight per square meter (except for pylon and landing gears). The Fig. 3 illustrates this for the fuselage

Examples of formula for mass estimation:

$$vtp\_mass = 25\, vtp\_area \tag{6}$$

$$htp\_mass = 22\, htp\_area \tag{7}$$

$$fuselage\_mass = 5.47 \left[\pi\, fuselage\_length \sqrt{fuselage\_width\, fuselage\_height}\right]^{1.2} \tag{8}$$

Concerning this last formula, the expression below the square root is the equivalent diameter of the fuselage. The expression between brackets is the fuselage skin area considered without any tapering, but is also proportional to the cabin floor area. In this case, the constant 5.47 cannot be interpreted as a mass per square meter for the whole structure because of the power 1.2. These values (factor 5.47 and exponent 1.2) has been found by regression using data and formulas coming from [9–16].

System mass and landing gear mass are driven by characteristic weights:

$$system\_mass = 0.545\, MTOW^{0.8} \tag{9}$$

$$ldg\_mass = 0.02\, MTOW^{1.03} + 0.012\, MLW \tag{10}$$

Pylon, nacelle and engine masses are driven by engine Sea Level Static Thrust (SLST):

$$pylon\_mass = 0.0031\, SLST\, n\_engine \tag{11}$$

$$nacelle\_mass = (1250 + 0.021\, SLST)\, n\_engine \tag{12}$$

Wing mass is taken from Shevel [14].

The core model chain contains the following 7 steps:

Fig. 3 Matter is distributed on surfaces, example of the fuselage

1) Initialization
2) Airframe predesign
3) Propulsion predesign
4) Mass and CG estimation
5) Nominal mission simulation
6) Operational performance estimation
7) Costs estimation

These steps are presented in the N2 diagram of Fig. 4. Not all the variables have been mentioned but only those responsible of the couplings that have to be solved during the design process. In order to improve lisibility, some packaging of the functions has been done:

- Individual component design functions have been gathered into two blocks: **Airframe_predesign** and **Propulsion_predesign**.
- All mass and center of gravity assessments have been packaged into the **Mass and CG estimation** block.
- All performance estimations are in the block called **Performances**.
- All criteria evaluations, especialy, economics and environmental are in the block **Criteria**.
- Finally, the box called **Weight balance** produces a new value of MTOW from Operating Weight Empty (OWE), payload and total mission fuel.

It should be noted that the coupling between airframe and propulsion predesigns must be solved to obtain a consistent geometrical description. In fact, this coupling is a little bit artificial because a pure sequential treatment could be implemented by merging airframe and propulsion predesign functions, but this possibility is only due to the simplicity of used internal formulas. In real life, different engineering teams are operating separately. It was decided to let this separation as an opportunity to experiment MDO processes.

The expression in italic about drag, thrust and Specific Fuel Consumption (SFC) stands for model functions that allow to compute these quantities in the various flight conditions required to simulate mission and evaluate operational performances.

This core model chain also shows some couplings between modules Mass, Nominal mission and Weight balance through MTOW, Maximum Zero Fuel Weight (MZFW) and MLW. The resolution of these couplings correspond to the so called Mass-Mission adaptation which consists in having exactly the right structural mass to carry the required payload and fuel for the nominal mission. An example of treatment is presented in the N2 diagram of Fig. 5.

An adequate solving process applied to this core model chain is able to produce consistent values of characteristic weights (MTOW, MLW, MZFW, OWE, and Manufacturer Weight Empty (MWE)) as well as operational performances (Take Off Field Length, Approach speed, Ceilings, Time to climb, . . .) and cost criteria (Cash Operating Cost, Direct Operating Cost). All tool ingredients are gathered to be able to optimize the initial airplane. Most common topmost

TLRs	propu_config n_engine	cruise_mach n_pax_ref	cruise_mach		design_range cruise_mach			
	Initialization	wing_area hld_type htp_attachment ...	ref_cruise_altp n_engine SLST BPR engine_attachment ...	MTOW MZFW MLW		Payload	*Operational requirements*	Economic assumptions
		Airframe preDesign	fuselage_width fuselage_height fuselage_length nacelle_x_axe	*Airframe geometry*	*Airframe drag*		*Airframe drag* *Airframe lift*	*Airframe drag* *Airframe lift*
		nacelle_y_axe nacelle_length	**Propulsion preDesign**	nacelle_mass pylon_mass	*Engine drag* *Engine thrust* *Engine SFC*		*Engine drag* *Engine thrust*	*Engine drag* *Engine thrust* *Engine SFC*
				Mass & Cg estimation		OWE MZFW MLW	MLW OWE	OWE MWE
					Nominal mission	fuel_total		
		MTOW		MTOW MZFW MLW	MTOW	**Weight balance**	MTOW	MTOW
							Operational Performances	
								Cost functions

Fig. 4 N2 diagram of the core model chain

design parameters are Wing area and Sea Level Static Thrust (reference_thrust which drives the engine size, thrust, consumption and weight through the parametric engine model).

To run this optimization process, it is just needed to input values to the topmost 3 TLRs (Design range, Cruise speed and passenger capacity), the two design options (propulsive architecture, number of engine) and to the following operational requirements:

1) Maximum take-off field length, sea level, ISA+15, MTOW
2) Maximum approach speed, sea level, ISA+15, MLW
3) Maximum time to climb to Top of Climb altitude, ISA, 97 % MTOW
4) Minimum climb speed at Top of Climb altitude, ISA, cruise Mach, 97 % MTOW, MCL rating
5) Minimum climb speed at Top of Climb altitude, ISA, cruise Mach, 97 % MTOW, MCR rating
6) Minimum air path at required One Engine Inoperative ceiling, ISA, best speed, 95 % MTOW, MCN rating

If the user does not know this requirements, initializing functions are available to propose acceptable values. The N2 diagram of Fig. 6 includes the performance optimization loop.

In addition to this core process, a very simple Handling Quality (HQ) library has been implemented which is focused on tail area sizing together with longitudinal positioning of the wing versus the fuselage. This operation is classically performed, for tube and wing arrangements, outside of the core process because it has normally limited impact on the overall design (wing positioning is a question of number of frame before and after the wing attachment and tail areas is normally a question of a few square meters from pre-design values). This HQ process evaluate only one single CG forward limit (trim at landing) and one single CG backward limit (static stability: margin versus neutral point) and tries to match these limits with max forward and max backward CG requirements produced by the CG function. The N2 diagram of the HQ process is presented on Fig. 7.

In real life, this last process is rather an optimization because there are many HQ constraints to satisfy and one never knows which ones will be active. Moreover, forward or backward CG active constraints may be different depending

propu_config n_engine n_pax design_range cruise_mach		cruise_mach n_pax_ref	cruise_mach		design_range cruise_mach n_pax	design_range cruise_mach			
Initialization	wing_area SLST	wing_aspect_ratio hld_type htp_attachment ...	ref_cruise_altp n_engine SLST BPR engine_attachment ...	MTOW MZFW MLW			Payload	*Operational requirements*	*Economic assumptions*
	PreDesign loop	nacelle_y_axe nacelle_length							
		Airframe preDesign	fuselage_width fuselage_height fuselage_length nacelle_x_axe		Airframe geometry	*Airframe drag*		*Airframe drag* *Airframe lift*	*Airframe drag* *Airframe lift*
	nacelle_y_axe nacelle_length		Propulsion preDesign		nacelle_mass pylon_mass	*Engine drag* *Engine thrust* *Engine SFC*		*Engine drag* *Engine thrust*	*Engine drag* *Engine thrust* *Engine SFC*
				Mass-Mission loop	MTOW MZFW MLW	MTOW		MTOW	MTOW
				MZFW MLW	Mass & Cg estimation		OWE	MLW OWE	OWE MWE
						Nominal mission	FuelTotal		
		MTOW		MTOW			Weight balance		
								Performances	
									Cost functions

Fig. 5 N2 diagram of the core process

on the mass of the aircraft which makes this process very tricky. Nevertheless, the great simplification that has been adopted reveals to be clever enough to improve tail sizing in comparison to volume based pre-sizing performed in Airframe predesign functions. The coupling of the HQ process to the core process can be done as shown on Fig. 8.

The overall process described above is a chain of a MDF process (performance optimization) with constraint satisfaction process (Tail re-sizing) into a fixed point overall loop. Experience shows that this scheme converges most of the time if we divide by 2 the changes in Vertical Tail Plane (VTP) area, Horizontal Tail Plane (HTP) area and wing position that are requested by the tail sizing step. Convergence is generally quite rapid (2 to 3 loops) but in some cases, it appears to be longer (more than 12 loops). The use of a fixed point scheme at this stage seems not very efficient, this way of doing has been selected just because it reflects some common practices. More efficient MDO strategies can surely be applied.

It is interesting to notice that the attempt to merge all constraint satisfaction sub-processes into a single one seems not to improve convergence in the difficult situations. At this stage, it is not possible to formally exclude the possibility of a bug, further investigations will be done to understand the causes of the problem. Nevertheless, it is to be noticed that tail sizing and wing positioning impact all disciplines through many causal loops. These multiple interactions may lead to difficulties to reach the optimum, especially when the domain around is very flat, which is the case here. It would be very interesting to test others MDO processes on this problem.

At the end of the process, it is possible to draw a simple 3 view drawing mainly for sanity check. The sketch shown on Fig. 9 is drawn into a 100m x 100m square to give an absolute perception of the size.

C. Examples of design

A few examples of design are presented in Table 2 and Fig. 10. These designs have been directly computed from top 3 inputs (range, speed, number of passengers) and the initialization functions. For all trials, design variables were *Wing area* and *engine size* and optimization criterion was *MTOW*. The yellow colored cells in the bottom of Table 2 indicate which constraints have been activated.

propu_config n_engine n_pax design_range cruise_mach			cruise_mach n_pax_ref	cruise_mach		design_range cruise_mach n_pax	design_range cruise_mach			
Initialization	wing_area SLST		wing_aspect_ratio hld_type htp_attachment ...	ref_cruise_altp n_engine SLST BPR engine_attachment ...	MTOW MZFW MLW			Payload	*Operational requirements*	*Economic assumptions*
	Performance optimization loop		wing_area	SLST						
		PreDesign loop	nacelle_y_axe nacelle_length							
			Airframe preDesign	fuselage_width fuselage_height fuselage_length nacelle_x_axe		Airframe geometry	*Airframe drag*		*Airframe drag* *Airframe lift*	*Airframe drag* *Airframe lift*
		nacelle_y_axe nacelle_length		Propulsion preDesign		nacelle_mass pylon_mass	*Engine drag* *Engine thrust* *Engine SFC*		*Engine drag* *Engine thrust*	*Engine drag* *Engine thrust* *Engine SFC*
					Mass-Mission loop	MTOW MZFW MLW	MTOW		MTOW	MTOW
					MZFW MLW	Mass & Cg estimation		OWE	MLW OWE	OWE MWE
							Nominal mission	FuelTotal		
			MTOW		MTOW			Weight balance		
	Operational constraints								Performances	
	Criterion ex: DOC									Cost functions

Fig. 6 N2 diagram of the performance optimisation

Pre-sizing	wing_x_root htp_area vtp_area	wing_area wing_aspect_ratio hld_type htp_type MTOW	MTOW MZFW MLW	Airframe drag Airframe lift Engine drag Engine thrust
wing_x_root htp_area vtp_area	Tail sizing	d_x_wing d_htp_area		
		Airframe preDesign	Airframe geometry	
	c_g_max_fwd_req c_g_max_bwd_req		Mass & Cg estimation	OWE
	max_fwd_cg_trim max_bwd_cg_stall	d_vtp_area		Handling Qualities

Fig. 7 N2 diagram of the HQ process

Note that initializing functions are making big decisions about airplane TLRs. Even if top 3 inputs correspond to existing design, other characteristics may be quite different because they do not match with other TLRs.

Finally, several gradient based optimizers from *Scipy.minimize* toolbox have been tried with various success (COBYLA, SLSQP, Trust-constr). Trust-constr has been finally selected with adapted pre-scaling of constraints and criteria. This setting seems to converge reasonably fast on most of the designs that have been proposed to it. A possible source of problem is probably the necessity to rely on finite differences to build the gradient of the functions, indeed, the module functions are using a lot of internal zero finding using *Scipy.minimize.f_solve* and basic settings which may introduce some numerical noise. If so, going to automatic differentiation may improve the situation. In any case, further

Table 2 Some automatic designs from MARILib

	unit	Airplane 1	Airplane 2	Airplane 3	Airplane 4	Airplane 5
Capacity		8	110	150	280	300
Range	NM	3300	3100	3000	6100	8000
Cruise Mach		0.79	0.78	0.78	0,82	0.85
SLST	daN	3200	9435	11795	31780	39485
BPR		5	9	9	9	9
Wing area	m^2	41,2	110,9	146,3	356,7	444,7
Span	m	19,3	31,6	36,3	56,7	63,3
Fuselage length	m	18.5	32,5	37.2	59,3	61,8
Fuselage width	m	2.4	3.5	3.9	5.7	5,7
MTOW	kg	17900	59380	76330	231290	298170
MLW	kg	17900	51260	67130	175680	209080
OWE	kg	11900	34710	44740	122180	150400
MWE	kg	11470	30930	39770	104260	125760
TOFL	m	1520	2000	2000	2795	3000
App Speed	kt	135	135,7	135,1	140	136,8
OEI path	%	1,8	1,8	1,9	1,3	1,2
Vz Climb MCL	ft/min	480	440	470	535	525
Vz Climb MCR	ft/min	0	60	90	180	170
TTC	min	22,4	25	25	25	25

investigations will be required to make automatic optimization more robust.

MARILib reveals to be quite robust exploring the design space from business jets to super jumbo, however, it remains possible to put the design process in a situation where it cannot start. This may happen when initializing functions are unable to propose a data configuration which can be evaluable by all sub models. In most of the case, it is possible to unlock the process by increasing the SLST proposed by the corresponding initialization function (as it is well known that "with big engines, you can fly anything. . . ").

Even if the set of TLRs matches perfectly an existing airplane, MARILib will, of course, not be able to retrieve the whole set of characteristics of the aircraft with high precision, this would reveal some sort of magic. But programmers may introduce shifts on the output of sub models to recover a known value. If enough reference data are available, the library can be tuned to reproduce the design of a reference aircraft and be used to assess some technological effects as the one which is proposed in the following of this paper.

If MARILib is not very precise to predict an existing design it can nevertheless be quite good as long as only differences between two designs are looked for.

Fig. 8 N2 diagram of the overall process

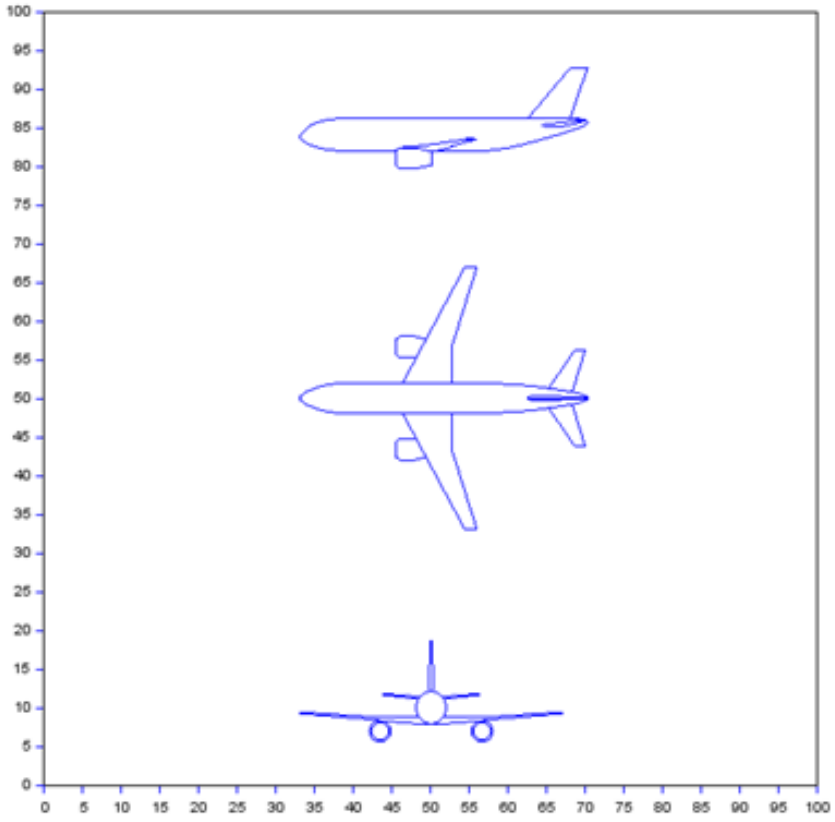

Fig. 9 Sanity check with 3 view drawing

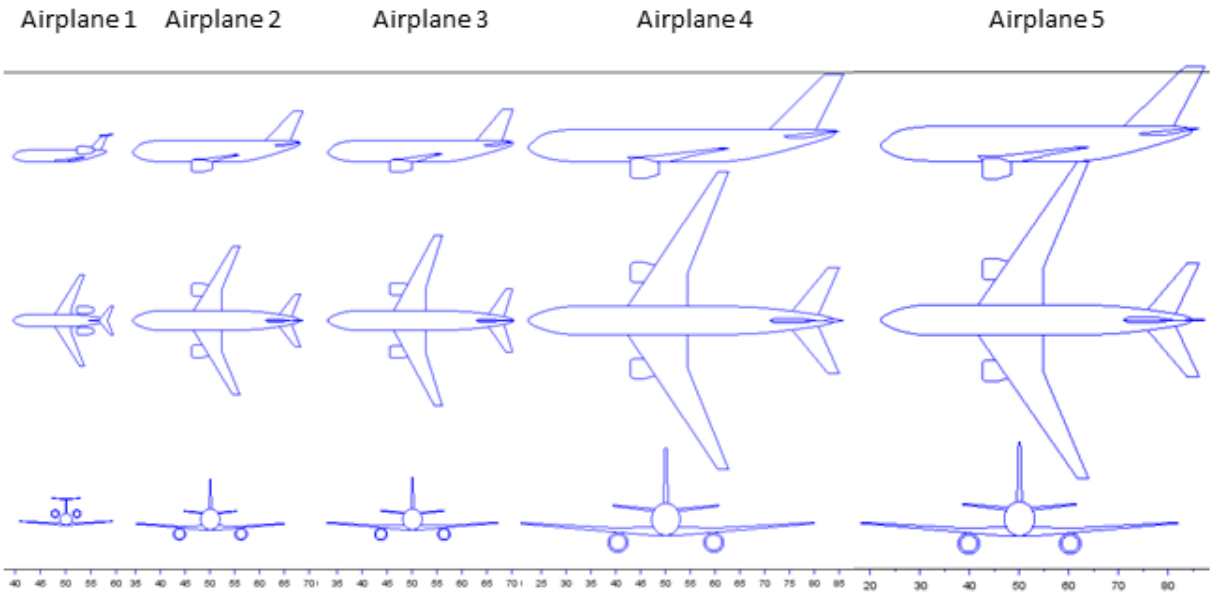

Fig. 10 3view drawing of the 5 airplanes

4. Hybrid architecture

It is proposed to use MARILib to experiment the possibility to model a hybrid architecture and to compare the performances of 2 configurations, one classical and one hybrid, optimized according to the same set of TLRs. The selected architecture, a partial turbo-electric, is described in Fig. 11.

A. Architecture definition

The reference aircraft is Airplane n°3 presented above. When components of an electric chain are added to a classical configuration, all new components are adding their weight and power loss and some of them are also adding drag. At the end of the chain, some thrust is produced that will not in itself compensate the additional weight, power loss and drag. As a result of this, the initial step of hybridization always reveals a loss in overall performance. To have a chance to decrease this loss or even to turn it into some benefit, the designer must take advantage of some specificities of electric devices. In the proposed arrangement, most important benefit is expected to come from the location of the electric fan at the rear end of the fuselage where it can ingest part (or totality) of the boundary layer. The boundary layer which is surrounding rear fuselage tail cone contains energy that have been dissipated on fuselage skin as drag and part of this energy can be recaptured for propulsion purpose.

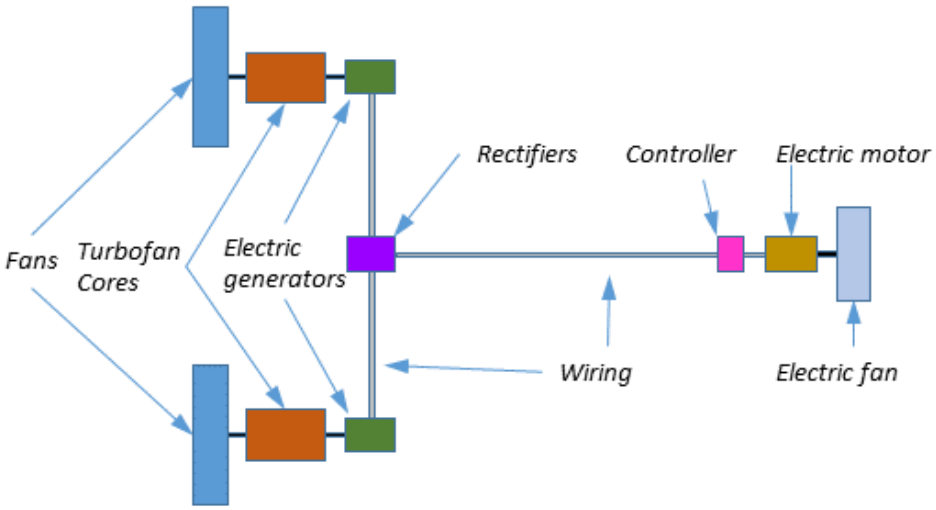

Fig. 11 Hybrid architecture

The weight of the components of the electric chain depend on the amount of power they have to manage. As a starting point, following assumptions have been taken for the power density of each type of component:

- **Generator**: 10 kW/kg,
- **Rectifier**: 20 kW/kg,
- **Wiring**: 20 kW/kg,
- **Cooling**: 15 kW/kg,
- **Controller**: 20 kW/kg,
- **Motor**: 10 kW/kg,
- **Fan and mounting**: 5 kW/kg.

The airplane which integrates this propulsive architecture could look like the NASA STARC ABL [17] presented in Fig. 12.

To model this kind of hybrid architecture, it is necessary to take into account all the main aspects of the electric chain and their impact on airplane performance. It is also necessary to quantify the benefit of the boundary layer ingestion. These models must be parametric so that they can play their role in the design process of the whole airplane. To make this possible, some strong assumptions have been taken. This has been done by considering some quantities as constants.

Before defining the model, it is interesting to recall what is at stake with the selected architecture: Ingesting the fuselage boundary layer is supposed to bring some benefit by recovering part of the energy dissipated as drag on the

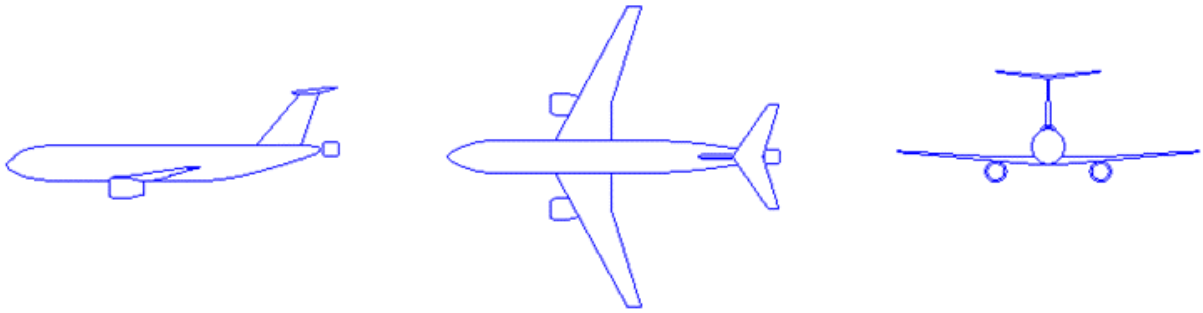

Fig. 12 Rear end fuselage mounted e-fan

fuselage skin. This energy is delivered around the fuselage as an air mass flow which has been dragged in the direction of the movement, the model must of course integrate this aspect. The main difficulty of Boundary Layer Ingestion (BLI) modelling is that drag and thrust interact tightly to produce an overall benefit which is hard to quantify without some complicated mathematics that are out of the scope of MARILib. Fortunately, the particular arrangement with an engine at the rear end of the fuselage can help to simplify the approach.

As the electric engine is plugged at most downstream position on the fuselage, the fuselage drag will be considered as unchanged except about tail cone drag (drag due to fuselage tapering) which may be reduced. As a consequence, only 2 phenomena can contribute to the benefit of the selected arrangement:

1) The reduction of fuselage tail cone drag
2) The kinetic energy captured by the inlet flow of the e-fan

The reduction of the fuselage tail cone drag is treated considering that the presence of the e-fan reduces the proportion of the cone wetted area which is generating this specific drag. This is really a rough model but we will take it at this stage. The principle and the notations are illustrated in Fig. 13.

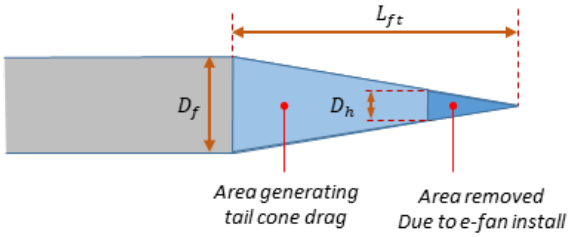

Fig. 13 Tail cone drag generating area

With a bit of geometry, the proportion K_a of remaining wetted area over total initial wetted area can be expressed as following:

$$K_a = 1 - \left(\frac{D_h}{D_f}\right)^2 \tag{13}$$

Consequently, remaining tail cone drag coefficient $Cd_{Cone\ BLI}$ can be estimated from clean fuselage coefficient Cd_{Cone} as following:

$$Cd_{ConeBLI} = Cd_{Cone}\left(1 - \left(\frac{D_h}{D_f}\right)^2\right) \tag{14}$$

The resulting benefit, with the geometry of the test case, is in the order of magnitude of 0.3 drag count which is very tiny, and perhaps pessimistic.

Basically, the e-fan that swallows part or totality of a boundary layer will take benefit of the global reduction of the inlet speed and jet speeds. To produce the same thrust as an e-fan working in free stream, it will use less power, or, with the same shaft power, it will produce more thrust. The reduction of the inlet speed depends on the inlet mass flow itself. If the mass flow is small, only the lower part of the boundary layer will be swallowed and the average speed reduction will be high. The resulting benefit will be high but the thrust produced will remain small. If the mass flow is important, the inlet will swallow a large part of the air outside of the boundary layer and the average speed reduction will be low. Then the benefit will be reduced but the thrust produced will be high. As we can see, best conditions cannot be found without optimizing the design of the e-fan. The model described below integrates these antagonist effects and allows looking for an optimal design.

B. Defining a hybrid SFC

The first objective is to find an expression of the SFC of a hybrid propulsive system from the characteristics of its components. The principle that has been applied is to start from a pure turbofan of a given size, weight, thrust and consumption (characterized by its SLST, By Pass Ratio (BPR) and its cruise SFC) and to derive from it a hybrid architecture introducing all necessary parameters to control the new components. The pure thermodynamic model is presented in the next chapter.

At big grain level, as shown in Fig. 14, a turbofan can be seen as 2 main components: a core and a fan coupled by a shaft. The whole system converts fuel flow into propulsive power with a given efficiency.

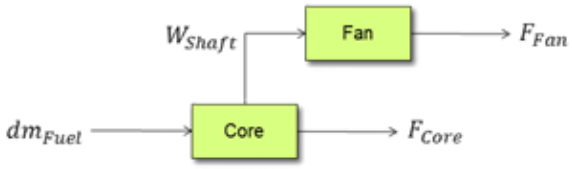

Fig. 14 Simplified architecture of a turbofan

The first big assumption will be to consider that the ratio $K_C = F_{Core}/(F_{Core} + F_{Fan})$ is constant and equal to about 13%. Actually, this ratio seems not to vary a lot in the whole flight domain (except in idle) for BPR higher or equal to about 5. With this assumption, it can be written:

$$F_{Core} = K_C(F_{Core} + F_{Fan}) \tag{15}$$

$$F_{Fan} = (1 - K_C)(F_{Core} + F_{Fan}) \tag{16}$$

What is classically called fan efficiency is the capability of the fan to convert shaft power into kinetic energy. This efficiency is here taken as a constant with a value corresponding to high efficiency fans:

$$\eta_x = \frac{\frac{1}{2}Q(V_{jet}^2 - V_{in}^2)}{W_{Shaft}} \approx 0.95 \tag{17}$$

For the purpose, a "propeller like" efficiency of the fan has been introduced with a value corresponding to highly efficient devices:

$$\eta_F = \frac{V_{Air}\, F_{Fan}}{W_{Shaft}} \approx 0.82 \tag{18}$$

These two efficiencies will be used in the following formulas to connect thrust, power and speed.

By definition:

$$\frac{dm_{Fuel}}{dt} = SFC_0(F_{Fan} + F_{Core}) \tag{19}$$

Combining Eqs. (15), (16), (18) and (19) gives:

$$W_{Shaft} = \frac{V_{Air}(1 - K_C)}{\eta_F \, SFC_0} \frac{dm_{Fuel}}{dt} \tag{20}$$

$$F_{Core} = \frac{K_C}{SFC_0} \frac{dm_{Fuel}}{dt} \tag{21}$$

All the elements are now in place to go to the next step which consists in deriving some power from the fan shaft to an electric generator. In normal operation (all engine operative) a simplification of the proposed partial turbo-electric architecture is shown on Fig. 15.

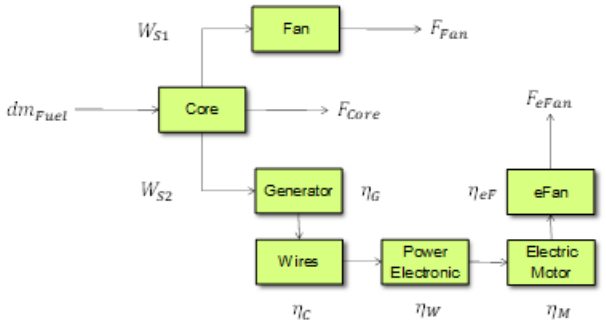

Fig. 15 Simplified partial turbo-electric architecture

Each component of the electric chain from the generator to the electric motor have its own efficiency. All these efficiencies can be merged into a single one. A value of 90% for this overall efficiency corresponds to a mean individual efficiency of each component of about 98% which is challenging:

$$\eta_E = \eta_G \eta_C \eta_W \eta_M \approx 0.90 \tag{22}$$

The factor K_W is now introduced: the ratio of the total power available on the fan shaft which is routed to the electric generator, this ratio will be a design parameter for the hybrid architecture:

$$W_{S2} = K_W(W_{S1} + W_{S2}) \tag{23}$$

$$W_{S1} = (1 - K_W)(W_{S1} + W_{S2}) \tag{24}$$

Combining Eqs. (18), (22), (23) and (24), gives:

$$F_{Fan} = \frac{\eta_F}{V_{Air}} W_{S1} = \frac{\eta_F (1 - K_W)(W_{S1} + W_{S2})}{V_{Air}} \tag{25}$$

$$F_{eFan} = \frac{\eta_{eF} \, \eta_E}{V_{Air}} W_{S2} = \frac{\eta_{eF} \, \eta_E \, K_W (W_{S1} + W_{S2})}{V_{Air}} \tag{26}$$

Combining Eqs. (20), (21), (25) and (26), produces:

$$F_{Fan} = \frac{(1 - K_W)(1 - K_C)}{SFC_0} \frac{dm_{Fuel}}{dt} \tag{27}$$

$$F_{eFan} = \frac{\eta_{eF} \, \eta_E \, K_W (1 - K_C)}{\eta_F \, SFC_0} \frac{dm_{Fuel}}{dt} \tag{28}$$

$$F_{Core} = \frac{K_C}{SFC_0} \frac{dm_{Fuel}}{dt} \tag{29}$$

Summing all the forces leads to:

$$F_{Core} + F_{Fan} + F_{eFan} = \frac{K_C\,\eta_F + (1-K_C)\,(\eta_{eF}\,\eta_E\,K_W + \eta_F(1-K_W))}{\eta_F\,SFC_0}\,\frac{dm_{Fuel}}{dt} \tag{30}$$

Finally:

$$F_{Core} + F_{Fan} + F_{eFan} = \frac{\eta_H}{SFC_0}\,\frac{dm_{Fuel}}{dt} \tag{31}$$

With:

$$\eta_H = K_C + (1-K_C)\left(\frac{\eta_{eF}}{\eta_F}\,\eta_E\,K_W + (1-K_W)\right) \tag{32}$$

We obtain an expression of the SFC of the hybrid architecture based on the SFC of a pure turbofan:

$$SFC_H = \frac{SFC_0}{K_C + (1-K_C)\left(\frac{\eta_{eF}}{\eta_F}\,\eta_E\,K_W + (1-K_W)\right)} \tag{33}$$

In fact, the turbofan which will be modified to drive a generator on its fan shaft will have approximately the same core but a reduced fan diameter, it will not be the same engine as the initial one, so that the term SFC_0 has no longer a clear signification.

A possible interpretation is that SFC_0 is a sort of **technological level**. From the point of view of the modified turbofan, it is the theoretical SFC of an engine without power offtake, which would have the same core, and which would have the adequate fan to absorb efficiently all the shaft power delivered by its core.

This expression of SFC_H allows to continue using Breguet equation for the hybrid airplane.

Additionally, it is possible to derive from Eqs. (16), (27), (28) and (29) a relation to compute the available power on the electric fan shaft from the total thrust F_0 of a classical turbofan without power offtake:

$$W_{eShaft} = V_{Air}\,\frac{\eta_E\,K_W + (1-K_W)}{\eta_F\,(K_c + (1-K_C)(1-K_W))}(F_{Core} + F_{Fan})_0 \tag{34}$$

Here again, the term $(F_{Fan} + F_{Core})_0$ is the theoretical thrust of an engine without power offtake, which would have the same core, and which would have the adequate fan to absorb efficiently all the shaft power delivered by its core.

It is to be noted that Eqs. (33) and (34) can be used on top of a model of pure turbofan, which is great regarding our objective of simplicity.

C. Definition of the initial turbofan engine

Pure turbofan engine model has been selected as simple as possible and is classical in the context of conceptual design. Thrust is globally scaled by the reference Sea Level Static Thrust (SLST) which is modulated by 3 factors:

$$Fn = SLST\,kFn_1(rating)\,kFn_2(BPR, Mach)\left(\frac{\rho}{\rho_0}\right)^{0.75} \tag{35}$$

1) kFn1 is a constant depending on engine rating

$$\begin{aligned}
&\text{if rating = MTO (Max Take Off)} && kFn_1 = 0.800,\\
&\text{if rating = MCN (Maxi Continuous)} && kFn_1 = 0.688,\\
&\text{if rating = MCL (Max CLimb)} && kFn_1 = 0.624,\\
&\text{if rating = MCR (Max Cruise)} && kFn_1 = 0.560,\\
&\text{if rating = FID (Flight Idle)} && kFn_1 = 0.100
\end{aligned} \tag{36}$$

2) kFn_2 is a factor that drives the thrust decrease versus Mach number and By Pass Ratio (BPR) according to a polynomial surrogate presented on Fig. 16. This surrogate has been established by running a simple thermo-mechanical engine model and varying BPR and Mach number.

$$kFn_2 = 0.475Mach^2 + 0.091\left(\frac{BPR}{10}\right)^2 - 0.283\left(\frac{BPR}{10}\right) - 0.663Mach - 0.081BPR + 1.192 \tag{37}$$

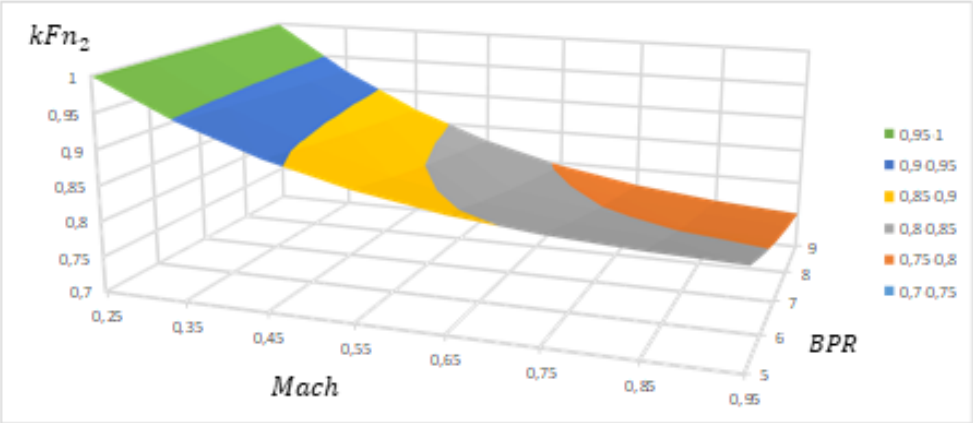

Fig. 16 Thrust dependence versus Mach and BPR

3) Finally, the term $\left(\frac{\rho}{\rho_0}\right)^{0.75}$ is driving the dependence of the thrust versus altitude

Fuel consumption is defined in cruise condition only by its Specific Fuel Consumption (SFC) as a regression versus BPR shown on Fig. 17.

$$SFC_0 = \left(0.4 + \frac{1}{BPR^{0.895}}\right)\left(\frac{1}{36000}\right) \tag{38}$$

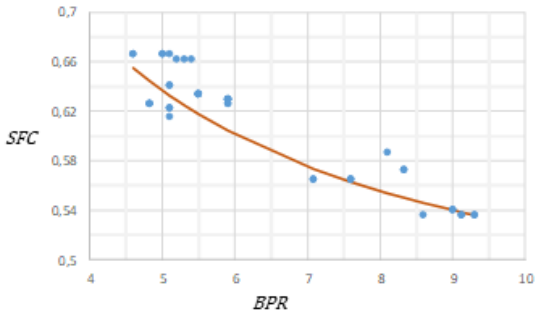

Fig. 17 SFC regression versus BPR

D. Derivation of a turbofan model

The engine with power offtake will have the same core but a reduced fan diameter. Considering that the air vein will be optimized for the new level of power, we consider that the fan efficiencies will remain unchanged. The new total thrust of the adapted engine is linked to the original thrust by:

$$K_{Fn} = \frac{Fn_1}{Fn_0} = K_C + (1 - K_C)(1 - K_W) \tag{39}$$

The diameter of the adapted fan can be calculated simply by applying the classical relation for engine scaling modified to take account of the diameter of the core which remain unchanged. To do so, we introduced K_D, the proportion of the total engine diameter which is taken by the core. In practice, this ratio depends on the BPR of the engine, we proposed the following formula extracted from measurements on several engine drawings:

$$K_D = 0.7 - 0.05(BPR - 5) \tag{40}$$

The classical formula for engine diameter is:

$$\frac{D_1}{D_0} = \sqrt{\frac{Fn_1}{Fn_0}} = \sqrt{K_{Fn}} \tag{41}$$

Adapted formula is:

$$\frac{D_1}{D_0} = \sqrt{K_{Fn}} + K_D(1 - \sqrt{K_{Fn}}) \tag{42}$$

The last aspect to be derived is the weight of the adapted engine with power offtake. Here again, a constant has been introduced to quantify the ratio of the core weight upon the total engine weight: $K_{\mathbf{M}}$. Due to a lack of available data, we retain the same expression as for K_D:

$$K_M = 0.7 - 0.05(BPR - 5) \tag{43}$$

The same approach as for the diameter has been adopted: start from the weight variation due to thrust decrease by using the weight estimation function of a pure turbofan and introduce on top the effect of an unchanged core:

Pure turbofan weight estimation:

$$M_{TF} = 1250 + 0.021 SLST \tag{44}$$

Basic weight ratio:

$$\frac{M_{TF1}}{M_{TF0}} = \frac{1250 + 0.021\, SLST\, K_{Fn}}{1250 + 0.021\, SLST} \tag{45}$$

Adapted weight ratio:

$$\frac{M_{TF2}}{M_{TF0}} = \frac{M_{TF1}}{M_{TF0}} + K_M(1 - \frac{M_{TF1}}{M_{TF0}}) \tag{46}$$

The constant coefficients that have been introduced to build this model of coupled turbofan and generator are assigned with the following values:

- $\eta_x \approx 0.95$,
- $\eta_F \approx 0.82$,
- $\eta_{eF} \approx \eta_F$,
- $K_C \approx 0.13$,
- $K_D \approx 0.7 - 0.05\ (BPR - 5)$,
- $K_M \approx 0.7 - 0.05\ (BPR - 5)$.

The variables that have been defined to drive the turbofan adapted with power offtake and reduced fan are:

- K_W,
- $SLST$,
- BPR.

These shifts of physical interpretation are not really a problem as overall effective $SLST$ and BPR can still be computed afterwards. Initial $SLST$ and BPR are just pure design variables of the hybrid configuration.

The effective $SLST_{hybrid}$ of the hybrid propulsion can be computed from the input variable $SLST$ as following:

$$SLST_{hybrid} = \left(\underbrace{K_C + (1 - K_C)(1 - K_W)}_{\text{Contribution of the turbofan}} + \underbrace{\frac{\eta_{eF}\, \eta_E\, K_W + (1 - K_W)}{\eta_F\, (K_C + (1 - K_C)(1 - K_W))}}_{\text{Contribution of the electric fan}} \right) SLST_0 \tag{47}$$

The effective BPR_{hybrid} of the hybrid propulsion must now be computed including the air flow going through the e-fan in the total cold flow.

E. Definition of the electric fan

The electric part of the architecture have now to be treated and more specially the design of the electric nacelle. The design principles are presented considering that the nacelle is in free air (without BLI). These design principles can be applied with or without BLI just by adapting air velocities and mass flows according to the boundary model presented in the next section.

Following quantities are looked for:
- D_{Fan},
- $D_{Nacelle}$,
- $L_{Nacelle}$,
- D_{Nozzle}.

Known data are:
- $Mach$,
- V_{Air},
- V_{snd},
- D_h,
- W_{eShaft},
- $\eta_x \approx 0.95$,
- $\eta_{eF} \approx 0.82$,
- Cp.

The definitions of η_x and η_{eF} give:

$$\eta_{eF} = \frac{V_{Air}\, F_{eFan}}{W_{eShaft}} = \eta_x \frac{V_{Air}\, Q\,(V_{jet} - V_{in})}{\frac{1}{2} Q\,(V_{jet}^2 - V_{in}^2)} = \eta_x \frac{2V_{Air}}{V_{jet} + V_{in}} \tag{48}$$

Noting $V_{jet} - V_{in} = \Delta V$ and making the assumption that $V_{in} = V_{Air}$ bring:

$$\frac{\eta_{eF}}{\eta_x} = \frac{2V_{Air}}{V_{jet} + V_{in}} = \frac{2V_{Air}}{2V_{Air} + \Delta V} = \frac{1}{1 + \frac{\Delta V}{2V_{Air}}} \tag{49}$$

From which ΔV can be obtained (about 75 m/s with proposed values of η_x and η_{eF}):

$$\Delta V = 2V_{Air} \left(\frac{\eta_x}{\eta_{eF}} - 1 \right) \tag{50}$$

The shaft power is converted into kinetic energy according to Eq. (51).

$$W_{eShaft}\, \eta_x = \frac{1}{2} Q\,(V_{jet}^2 - V_{in}^2) \tag{51}$$

Using Eqs. (50) and (51) gives:

$$Q = \frac{W_{eShaft}\, \eta_x}{2V_{Air}^2 \frac{\eta_x}{\eta_{eF}} \left(\frac{\eta_x}{\eta_{eF}} - 1 \right)} \tag{52}$$

Stagnation pressure and temperature at air inlet are given by:

$$P_{stag} = P_{amb} \left(1 + \frac{\gamma - 1}{2} Mach^2 \right)^{\frac{\gamma}{\gamma - 1}} \tag{53}$$

$$T_{stag} = T_{amb} \left(1 + \frac{\gamma - 1}{2} Mach^2 \right) \tag{54}$$

The Mach number at fan input, $Mach_{fan}$, is taken equal to 0.5 which is a classical design rule for air inlet. The corrected air flow per area gives a relation between mass flow and section:

$$\frac{Q}{A_{Fan}} = \frac{P_{stag}}{\sqrt{T_{stag}}} \sqrt{\frac{\gamma}{R}} \frac{Mach_{fan}}{\left(1 + \frac{\gamma-1}{2} Mach_{fan}^2\right)^{\frac{\gamma+1}{2(\gamma-1)}}} \tag{55}$$

From which the area of the e-fan vein section can be obtained:

$$A_{Fan} = Q \frac{\sqrt{T_{stag}}}{P_{stag}} \sqrt{\frac{R}{\gamma}} \frac{\left(1 + \frac{\gamma-1}{2} Mach_{fan}^2\right)^{\frac{\gamma+1}{2(\gamma-1)}}}{Mach_{fan}} \tag{56}$$

Considering the diameter of the hub, the diameter of the fan is:

$$D_{Fan} = \sqrt{D_h^2 + \frac{4}{\pi} A_{Fan}} \tag{57}$$

The nacelle diameter $D_{Nacelle}$ is deduced from D_{Fan} taking into account a necessary structural thickness around the fan:

$$D_{Nacelle} = 1.20\, D_{Fan} \tag{58}$$

The nacelle length $L_{Nacelle}$ is deduced from $D_{Nacelle}$ as follows:

$$L_{Nacelle} = 1.5\, D_{Nacelle} \tag{59}$$

Nozzle diameter is computed the same way as fan diameter but considering the exhaust velocity.

$$V_{jet} = V_{air} + \Delta V \tag{60}$$

Stagnation temperature after the fan can be calculated as following:

$$T_{stag_{jet}} = T_{stag} + \frac{W_{eShaft}}{Q\, Cp} \tag{61}$$

Static temperature is now:

$$T_{stat} = T_{stag_{jet}} - \frac{V_{jet}^2}{2Cp} \tag{62}$$

From which sound velocity can be obtained by:

$$V_{sndjet} = \sqrt{\gamma\, R\, T_{stat}} \tag{63}$$

Which leads to:

$$Mach_{jet} = \frac{V_{jet}}{V_{sndjet}} \tag{64}$$

Finally, stagnation pressure can be computed at nozzle exhaust considering that gas expansion is continued until ambient pressure:

$$P_{stag_{jet}} = P_{amb} \left(1 + \frac{\gamma - 1}{2} Mach_{jet}^2\right)^{\frac{\gamma}{\gamma-1}} \tag{65}$$

All quantities are now available to compute the nozzle area:

$$A_{Nozzle} = Q \frac{\sqrt{T_{stag_{jet}}}}{P_{stag_{jet}}} \sqrt{\frac{R}{\gamma}} \frac{\left(1 + \frac{\gamma-1}{2} Mach_{jet}^2\right)^{\frac{\gamma+1}{2(\gamma-1)}}}{Mach_{jet}} \tag{66}$$

And finally:

$$D_{Nozzle} = \sqrt{\frac{4}{\pi} A_{Nozzle}} \tag{67}$$

All required elements are now available to be able to compute off design working point of the electric fan. Before this, the model of boundary layer is presented as it is used for of design e-fan computations.

F. Model of the boundary layer

Many things have been written about Boundary layer ingestion and its benefit for air transport efficiency. Here, we do not pretend to propose precise approach to model BLI but just a simple one, only based on most important aspects of the phenomenon.

The thickness of a turbulent boundary layer which develops over a flat surface is classically given by Eq. (68).

$$\delta = \frac{0.385\, L}{(Re\, L)^{\frac{1}{5}}} \tag{68}$$

Where Re is the Reynold's number per length unit and L is the distance from which the boundary layer develops, δ is the height above the surface at which air longitudinal velocity has reached 99% of free stream velocity.

The longitudinal velocity, in airplane frame, at y height above the surface is given by Eq. (69) and illustrated on Fig. 18 and Fig. 19.

$$v = V_{Air} \left(\frac{y}{\delta}\right)^{\frac{1}{7}} \tag{69}$$

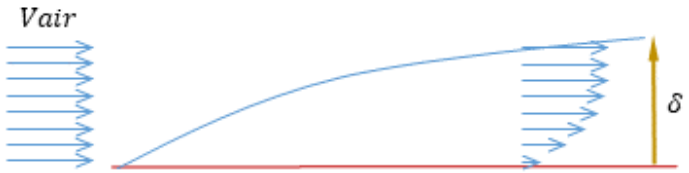

Fig. 18 Boundary layer velocity profile in airplane frame

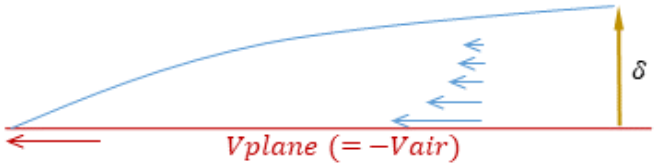

Fig. 19 Boundary layer velocity profile in ground frame

The problem is to model the shape of the boundary layer in front of the e-fan. The geometry of the fuselage rear end is a bit complicated, with a non-symmetrical necking immersed into the downwash of the wing, a complicated air flow structure can be expected at this place. At least, no full 3D description of the flow is required but a mean axisymmetric model. The model presented below has been built using mass flow considerations.

The drawing number 1 of Fig. 20 presents the target arrangement to model. Assessing the thickness and velocity profile of the resulting boundary layer at e-fan input, has been done in two steps as illustrated on Fig. 20:

1) Using Eq. (68), compute the boundary layer thickness δ_0 of the theoretical fuselage of drawing n°2 at the same longitudinal position of the e-fan inlet of drawing n°1. In ground frame, according to Eq. (69), this boundary layer contains a certain mass flow Q_{BL}, e.g. all the air mass which is dragged by the moving fuselage (presented in blue).

2) Compute the thickness δ_1 of the boundary layer, of the same velocity profile (Eq. (69)), which will pass the same mass flow Q_{BL} around the hub of the e-fan, as illustrated on drawing number 3 of Fig. 20. The resulting boundary layer thickness is of course greater, i.e. $\delta_0 < \delta_1$.

The resulting air velocity profile is used to compute the mass flow averaged velocity V_{BL} which is swallowed by the e-fan according to its dimensions, power and flying conditions.

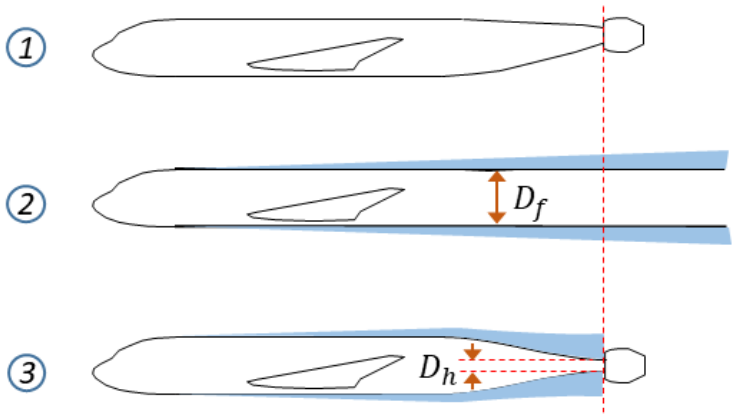

Fig. 20 Boundary layer thickness at e-fan inlet

Fuselage diameter D_f and hub diameter D_h being given, it is possible to compute δ_1 as a function of δ_0 independently from any other data. The resulting curve is presented on Fig. 21.

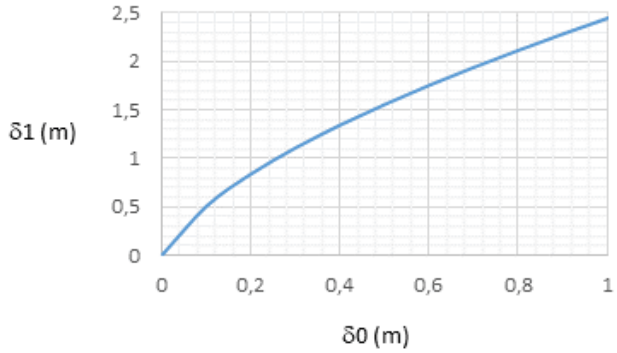

Fig. 21 Boundary layer thickness at e-fan inlet versus theoretical thickness on fuselage wall

The difference between mass flow averaged air velocity and the free stream air velocity $V_{Air} - V_{BL}(y)$ can be computed versus the captured air flow around the hub $Q_{BL}(y)$ as shown in Eq. (70) where y is the thickness of the air ring around the hub which is swallowed by the e-fan. Figure 22 illustrates this situation. This theoretical curve has been compared versus a curve obtained by post-treatment of a RANS computation on a similar geometry. The comparison is presented on Fig. 23 which shows no significant differences at the targeted level of precision.

$$\frac{V_{Air}}{V_{BL}(y)} = \frac{Q_{Free\ Stream}(y)}{Q_{BL}(y)} \tag{70}$$

G. Off design behavior of the electric fan

Supposing the e-fan has been designed according to the process presented above, another process to simulate its behavior inside the rear fuselage wake in all the flight domain must be put in place.

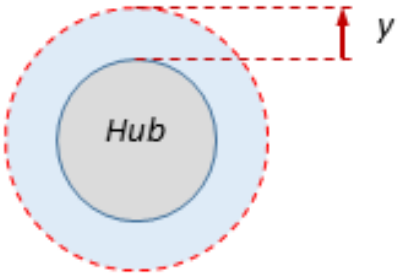

Fig. 22 Air ring swallowed by the e-fan

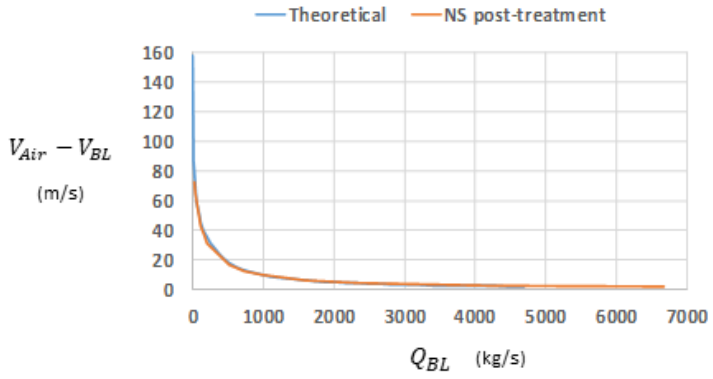

Fig. 23 Comparison Theory - RANS

We want to compute Fn_{eFan}.
Known data are:

- $\eta_x \approx 0.95$,
- $\eta_F \approx 0.82$,
- $\eta_{eF} \approx \eta_F$,
- $\eta_E \approx 0.90$,
- $K_C \approx 0.13$,
- K_W,
- D_f,
- D_h,
- D_{Nozzle},
- W_{Shaft},
- $Mach$,
- V_{Air},
- V_{snd}.

A 3 steps approach has been selected:

1) Calculate the theoretical boundary layer thickness δ_0 of a virtual fuselage of constant diameter and interpolate δ_1 in the precomputed curve (see Fig. 21).
2) Calculate the thickness of the air ring swallowed by the e-fan according to the available power on the e-fan shaft and deduce the mass flow Q_{eFan} across the e-fan and air speeds at inlet (V_{BL}) and jet (V_{jet}). This is done according to the process presented below.
3) Calculate the resulting e-fan thrust with:

$$Fn_{eFan} = Q_{eFan}(V_{jet} - V_{BL}) \tag{71}$$

The process to compute air flow characteristics across the e-fan is looking for the thickness y of the air ring that enters the e-fan inlet. To find this thickness, a function is built to get y as input and produce a residual which must be driven to zero. This solving is managed by a math library function, here, only the skeleton of the function is presented.

1) From D_f, D_h, $\delta 1$ and y, calculate the captured air flow $Q_{BL}(y)$ and the mass flow averaged air flow speed loss dV_{BL} using Eqs. (69) and (70).

2) Calculate inlet air speed $V_{BL}(y)$:
$$V_{BL}(y) = V_{Air} - dV_{BL}(y) \tag{72}$$

3) From W_{eShaft} calculate $Mach_{jet}$ the same way that have been used for e-fan design:
$$V_{jet}(y) = \sqrt{\frac{2\,W_{eShaft}}{Q_{BL}(y)} + (V_{Air} - dV_{BL}(y))^2} \tag{73}$$
$$T_{stag_{jet}} = T_{stag} + \frac{W_{eShaft}}{Q_{BL}(y)\,Cp} \tag{74}$$
$$T_{stat\,jet} = T_{stag_{jet}} - \frac{V_{jet}(y)^2}{2Cp} \tag{75}$$
$$V_{snd\,jet} = \sqrt{\gamma\,R\,T_{stat\,jet}} \tag{76}$$
$$Mach_{jet}(y) = \frac{V_{jet}(y)}{V_{snd\,jet}} \tag{77}$$

4) From D_{Nozzle} calculate the air mass flow across the nozzle
$$P_{stag} = P_{amb}\left(1 + \frac{\gamma - 1}{2} Mach_{jet}^2\right)^{\frac{\gamma}{\gamma-1}} \tag{78}$$
$$Q'_{BL}(y) = D_{Nozzle}\frac{P_{stag}}{\sqrt{T_{stag}}}\sqrt{\frac{\gamma}{R}}\,\frac{Mach_{jet}(y)}{\left(1 + \frac{\gamma-1}{2} Mach_{jet}(y)^2\right)^{\frac{\gamma+1}{2(\gamma-1)}}} \tag{79}$$

The solver must then find y so that $Q'_{BL}(y)$ equal to $Q_{BL}(y)$.

H. Effect of BLI on fuel consumption

Thanks to previous development, it is possible to calculate total thrust of the propulsive hybrid architecture but to be able to compute used fuel during missions, we must also determine the impact of BLI on fuel consumption. This can be done by modifying Eq. (18) and more particularly, by changing the signification of η_{eF}.

$$\eta_{eF} = \frac{V_{Air}\,F_{eFan}}{W_{eShaft}} \tag{80}$$

Originally, η_{eF} is an efficiency but it also quantifies the thrust that can be obtained by the $eFan$ from a given mechanical power W_{eShaft} at a given speed V. Just sticking to this definition, the factor K_{BLI} is introduced to give the relative $eFan$ thrust increase due to BLI. K_{BLI} can be obtained by virtually running the e-fan with and without boundary layer ingestion, in cruise condition, and do the ratio of the obtained thrusts.

Finally:
$$F_{eFan} = \frac{\eta_{eF}\,K_{BLI}\,W_{eShaft}}{V} \tag{81}$$

In Eq. (33), η_{eF} just have to be replaced by the product $\eta_{eF}\,K_{BLI}$ to introduce the effect of BLI on overall consumption.

Table 3 e-chain design versus installed electric power

	unit	0.05MW	0.25MW	0.5MW	0.75MW	1.MW	1.25MW	1.5MW	1.75MW	2.MW
L_{Fan}	m	1,05	1,43	1,76	2,02	2,25	2,44	2,62	2,79	2,94
D_{Fan}	m	0.58	0.80	0.98	1.12	1.25	1.36	1.46	1.55	1.63
D_{Nozzle}	m	0.26	0.50	0.68	0.80	0.91	1,0	1.08	1.16	1.23
dV_{BLI}/V_{Air}	-	0.45	0.34	0.29	0.27	0.25	0.23	0.22	0.20	0.196
K_{BLI}	-	1.50	1.33	1.27	1.23	1.21	1.19	1.18	1.17	1.16
K_{SFC}	-	0.9985	0.996	0.994	0.993	0.992	0.992	0.992	0.992	0.993
e-chain mass	kg	31	154	308	463	617	771	925	1079	1233

$$SFC_H = \frac{SFC_0}{K_C + (1 - K_C)\left(\frac{\eta_{eF} K_{BLI}}{\eta_F}\eta_E K_W + (1 - K_W)\right)} \tag{82}$$

It is to be noted that the product $\eta_{eF} K_{BLI}$ is no longer an efficiency, it can be higher than 1 because the limit of the studied system has been changed (the speed "seen" by the fan is different from V_{Air}).

Table 3 summarizes the evolution of some important parameters when varying the mechanical power of the electric motor.

When shaft power varies from 50kW to 2MW, one can observe that:

1) Inlet velocity loss varies from about 45% to 20% of the free stream velocity.
2) The e-fan thrust is from about 50% to 15% higher than in free stream.
3) The SFC improves from about 0.15% to 0.8% with a plateau of maximum effect between 1 MW and 1.75MW.

Considering these first results, it seems that we may expect no more than about 1 % benefit in SFC with this type of architecture but we must integrate all the other aspects and more especially weight. Thanks to the modelling principles described below, we have all bricks in hand to solve a complete design problem.

5. Some results from design process

The reference airplane is the Airplane 3 of Table 2. Presented values of fuel consumption and Cash Operating Cost have been computed on a 800NM mission. A first optimization has been done according to the same set of TLRs as Airplane 3 and the comparison with Airplane 3 is presented below. Additionally, some sensitivity studies have been done to experiment the behavior of the implementation of partial turbo-electric model into MARILib. The process presented in Fig. 6 has been played for all the following trials. It is to be noticed that in order to accelerate the convergence of the optimization, handling quality modules have not been used for empennage sizing. Empennage sizes have been determined through constant volume coefficients.

A. Optimization of a partial turboelectric

As fuel consumption reduction is an objective when dealing with hybrid architecture, the block fuel on 800NM mission has been used as an optimization criterion for all following computations. The e-fan power has been set to 1 MW for a first attempt and the wing area and engine size have been optimized to minimize block fuel for both classical and hybrid configurations. The main results are presented in Table 4.

At 1 MW e-fan power, we can see that the overall benefit in term of block fuel is very marginal (-0.16%). The next set of trials will try to look for the optimal e-fan power.

The present result can nevertheless be explained by the fact that the downsizing of the fan of the turbofans produces a benefit of 270kg, which does not compensate the additional 620kg of the overall electric chain. Furthermore, the new

Table 4 Comparison between classical and 1 MW hybrid aircraft

	unit	Airplane 3	Hybrid	Relative difference
Capacity	seat	150	150	-
Range	NM	3000	3000	-
Cruise Mach	-	0.78	0.78	-
Overall SLST	daN	11460	11300	-1,4%
Turbofan mass	kg	7500	7230	-3,6%
e-fan power	kW	-	1MW	
Electric chain mass	kg	-	620	
Wing area	m^2	151,9	152,9	+0,66%
Span	m	37	37,1	+0,27%
Fuselage length	m	37.2	37,2	
Fuselage width	m	3.9	3,9	
MTOW	kg	76840	77210	+0,48%
MLW	kg	67700	68130	+0,64%
OWE	kg	45270	45670	+0,88%
MWE	kg	40300	40710	+1,02%
Cruise SFC	Kg/daN/h	0.5399	0.5355	-0,81%
Cruise L/D	-	18.32	18,31	-0,22%
TOFL	m	1930	1970	+2,07%
App Speed	Kt	133,2	133,1	-0,08%
OEI path	%	2,0	1,8	-10%
Vz Climb MCL	ft/min	470	470	-
Vz Climb MCR	ft/min	90	100	+11%
TTC	min	25	25	-
Block Fuel 800NM	Kg	3701	3695	-0,16%
COC 800NM	$/trip	9892	9891	-0,01%
CO2 metric	10^{-7}Kg/km/$m^{0.48}$	7774	7752	-0,28%

optimum requires an increase of the wing area by $1m^2$, which results in an overall increase of about 400kg of the MWE. Finally, as the L/D in cruise remains roughly stable, the 0.8% benefit in SFC are vanished by the MWE increase.

This first result is a bit disappointing but up to now, the e-fan power has not been optimized. This is the objective of the next step of this short study.

B. Effect of e-fan power

The power of the e-fan electric motor has been varied from 50kW to 4MW. Only the graphics are presented on Fig. 24 but more extensive data are in the Table 5, Table 6, and Table 7 presented in appendix. Graphics have been drawn for three criteria: Block fuel, Cash Operating Cost (COC), CO_2 metric and three physical characteristics of the airplane: overall propulsion mass, cruise SFC and L/D. An optimal e-fan power of about 250kW is clearly visible on the curves, sadly, the overall benefit in term of block fuel for instance is about 0.6%. The lift to drag ratio experiments a small variation with a curious minimum at about 1.75 MW which is due to the competing evolution of wetted area versus wing area but this variation is not the main ingredient of the global result. The specific fuel consumption shows a clear minimum at about 1.5 MW but the benefit culminates at about 0.85% which is barely enough to compensate the increase of the propulsion system mass for low values of e-fan power. With the assumptions that have been taken, it seems that the presented hybrid configuration shows a margin benefit in the range of 1% in term of bloc fuel. Of course, at this stage, one cannot exclude the possibility of an over simplification or even a bug somewhere in the library.

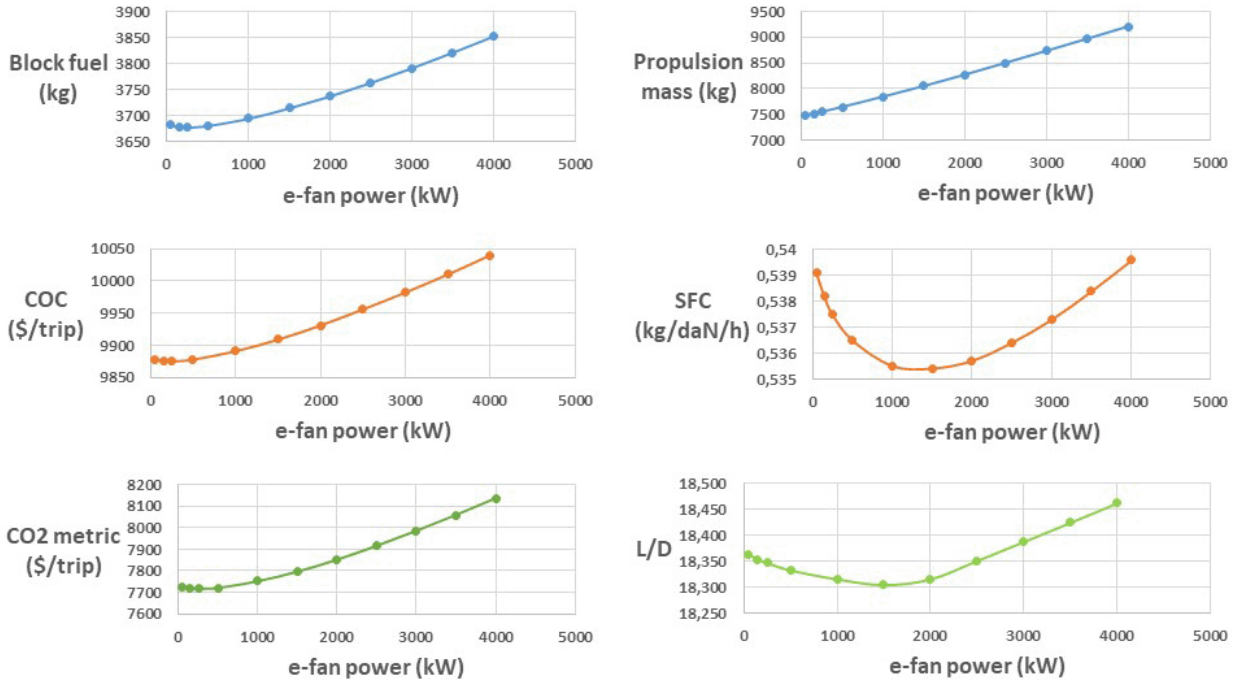

Fig. 24 Effect of e-fan power with basic assumptions

C. Effect of electric chain efficiency

For this test, electric chain efficiency has been increased from 90% to 95%, which corresponds to a mean component efficiency of about 99% for the components of the electric chain. Installed electric power has been varied in the same range as previously. Results are presented in Fig. 25.

The global behavior is similar to what has been obtained in the previous study but here the benefit in term of block fuel is obtained at about 500 kW and is raising 0.8%. The main difference seems to come from the SFC which shows a benefit of about 1.5% for an e-fan power of about 3.5 MW.

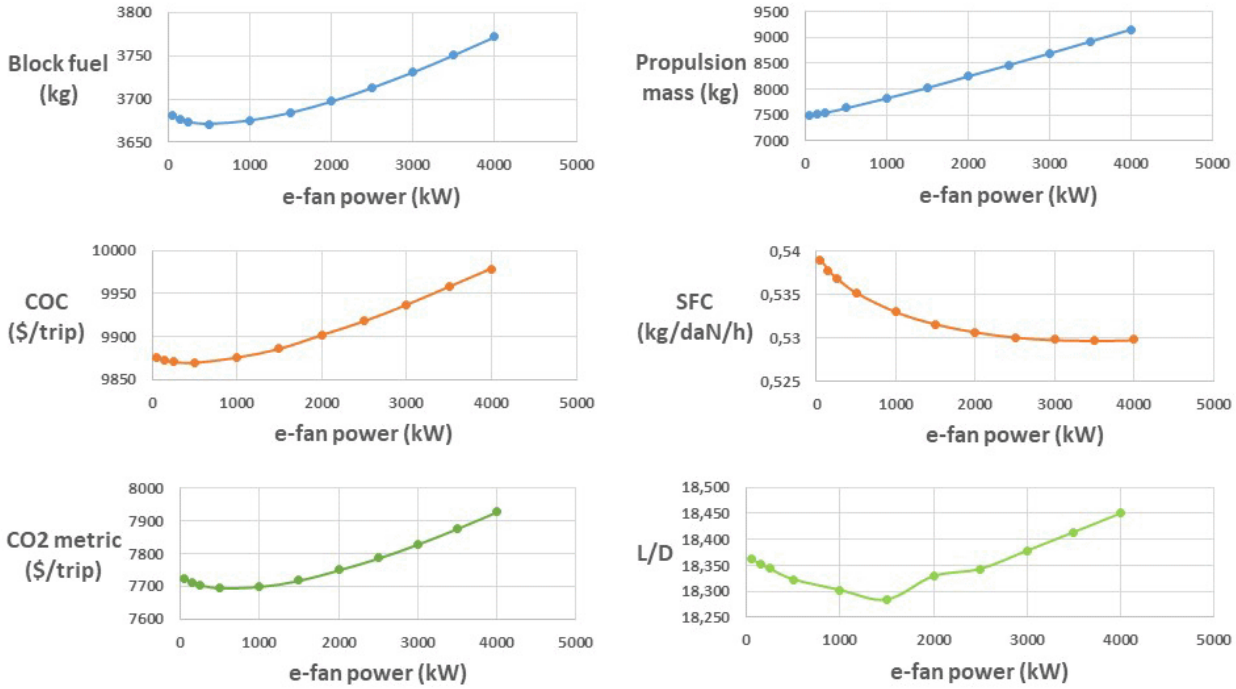

Fig. 25 Effect of e-fan power with electric chain efficiency at 95%

D. Electric chain power density

For this last test, power density of all components of the electric chain have been doubled compared to those presented in paragraphs 5.1, 5.2, 5.3, which would be an achievable challenge, even if the e-chain mass for low e-fan power seems a bit optimistic. The results of this last test are presented on Fig. 26.

In this case also, benefit of hybridization remains margin and only appears for limited electric power of about 1.5 MW. Maximum SFC benefit appears at 3.5 MW and is about 1.5%. COC benefit is not significant and maximum fuel reduction is close to 1%.

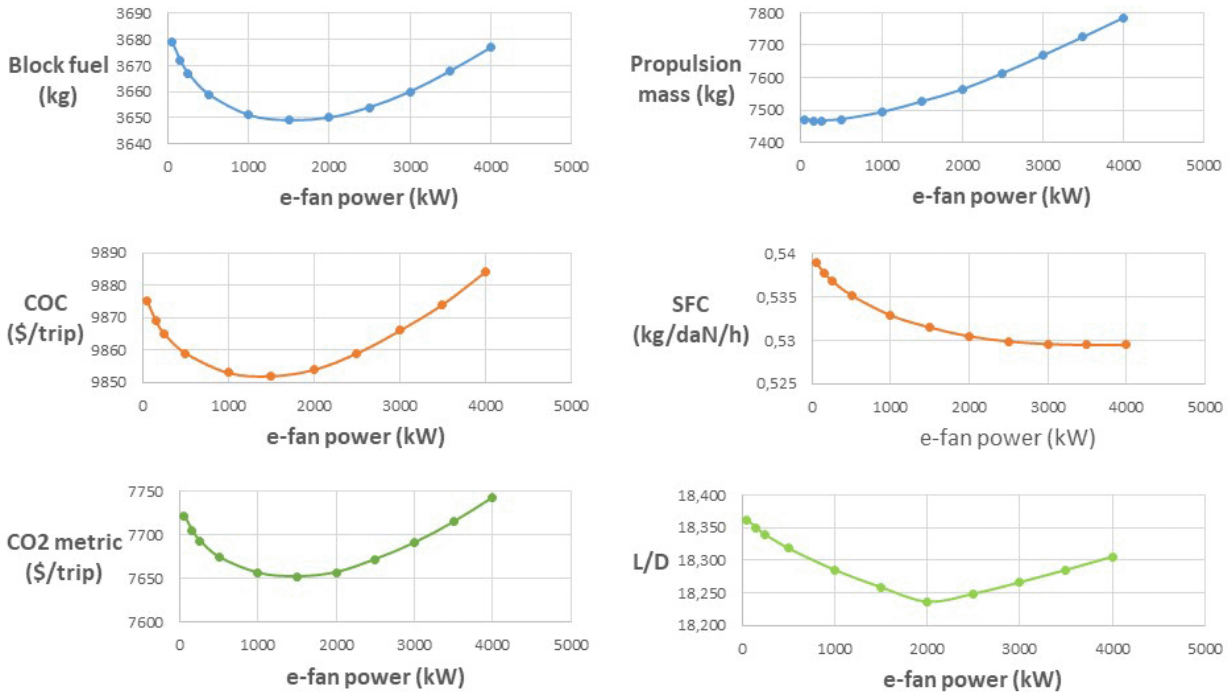

Fig. 26 Effect of e-fan power with electric chain efficiency at 95% and power density doubled

E. Conclusion

The presented short study seems to be in line with the results already obtained [17] which is that maximum benefit of a partial turboelectric architecture with boundary layer ingestion installed on a short range airplane is obtained with an installed electrical power of about 1MW to 3MW.

Nevertheless, a specific result of the presented study is that the overall benefit in term of block fuel that can be obtained is quite low and is in the order of magnitude of 1%. But further testing of the library is required to validate such result.

6. Interfacing with the GEMS MDO library

GEMS is a MDO framework, which offers many possibilities to build, run and post process complex multidisciplinary design problems based on a catalog of MDO formulations [7] [8].

Connecting software modules to a platform can be very challenging if some automatic capabilities are not in place to facilitate the work. A mechanism has been put in place to automatically identify the inputs and outputs of MARIlib functions, and generate the corresponding wrappers. All MARIlib functions read their inputs in the Aircraft object data structure, and also write their outputs to it. Python's introspection mechanisms are used to detect the read and write access to the Aircraft attributes, and then generate GEMS' interface to it. To use this mechanism one has to build a runnable sequence of call to the functions to be wrapped to GEMS. Then, the GEMS Discipline's interface can be generated. It is assumed that the data context of the run activates the internal parts of the functions that are targeted for future work with GEMS.

An example of sequence of treatments, were each call is packaging one or more MARILib functions is provided below.

```
aircraft = Aircraft()
n_pax_ref = 150                    # Reference number of passengers
design_range = unit.m_NM(3000)     # Design range
cruise_mach = 0.78                 # Nominal cruise mach number
propu_config = 1                   # 1: turbofan, 2: partial turbo electric
n_engine = 2                       # Number of engine
aircraft_initialization(aircraft,
```

```
                        n_pax_ref,
                        design_range,
                        cruise_mach,
                        propu_config,
                        n_engine)
fuselage_design(aircraft)
predesign_initialization(aircraft)
lifting_plane_design(aircraft)
propulsion(aircraft)
aircraft_aerodynamics(aircraft)
aircraft_mass(aircraft)
nominal_mission(aircraft)
mass_coupling(aircraft)
performance_analysis(aircraft)
payload_range_analysis(aircraft)
criteria(aircraft)
```

This sequence can be run as is, since all necessary inputs along it are computed by upper steps or initialized by dedicated functions. It is the only input required by to build the suitable GEMS wrapper around each function. Afterwards, an N2 diagram can be drawn in order to check the effective dependencies between the functions. If dependencies are correct, the approach allows to manage any design problem that can be built using the functions of the initial sequence according to a user selected solving process like IDF or MDF as illustrated in Fig. 27. Therefore, the OAD design problems can be addressed through the wide range of MDO formulations, optimization, DOE, surrogate models and coupling algorithms available in GEMS.

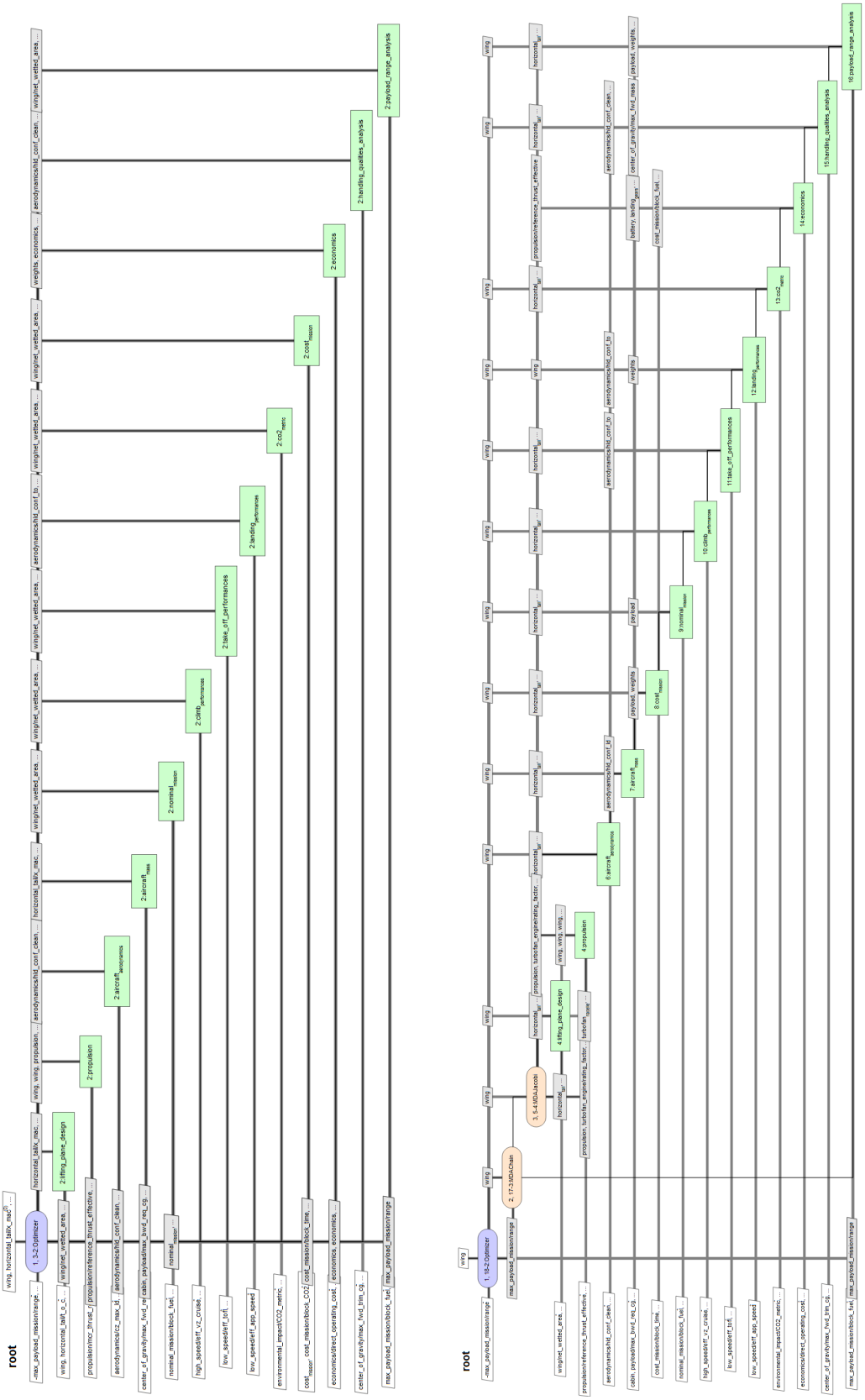

(a) IDF formulation (b) MDF formulation

Fig. 27 Examples of MDF and IDS XDSM diagrams of GEMS processes generated from MARIlib functions

7. Conclusion

This paper has introduced MARILib software (**M**ultidisciplinary **A**irplane **R**esearch **I**ntegrated **Lib**rary). The models in MARILib are globally much simpler than models that can be found in other aircraft conceptual design software but they revealed to be quite robust in finding the relevant order of magnitude of aircraft definition in a wide range of designs. The library can be used to experiment MDO strategies, generate consistent starting point for aircraft design studies and also be an easy to use playground for teaching activities in the field of conceptual aircraft design. For experienced users, MARILib can also be a laboratory to develop and experiment simple models as the partial turbo-electric with boundary layer ingestion which have been presented and couple them with an airplane design process. As a side effect, the propulsion hybridization introduces many new design parameters which makes more complex the overall design problem and give more opportunities to test MDO strategies. Finally, an automatic interfacing of MARILib with the GEMS MDO library has been illustrated. MARILib will be available as Open Source.

Appendix

More extensive results from effect of e-fan power analysis

Table 5 Effect of e-fan power with electric chain efficiency at 95% - (a)

e-fan power	MW	-	0.05	0.15	0,25	0,5	1,0	1,5	2,0	2,5	3,0	3,5	4,0
e-chain mass	kg	-	31	93	154	308	617	925	1233	1542	1850	2158	2467
Effective ref thrust	daN	11460	11401	11382	11367	11341	11307	11286	11285	11306	11330	11359	11391
Turbofan nacelle mass	kg	7500	7459	7428	7400	7339	7229	7128	7038	6959	6883	6810	6739
Propulsion mass	kg	7500	7490	7521	7554	7647	7846	8053	8271	8501	8733	8968	9206
Wing area	m^2	151,9	152	152	152,1	152,3	153	153,8	155,3	157,7	160,1	162,6	165,1
MTOW	kg	76840	76669	76686	76724	76858	77211	77618	78121	78722	79344	79981	80634
MLW	kg	67700	67615	67647	67692	67823	68133	68470	68893	69410	69937	70473	71017
OWE	kg	45270	45191	45222	45264	45386	45675	45991	46386	46869	47362	47863	48371
MWE	kg	40300	40227	40258	40300	40422	40711	41027	41422	41905	42398	42899	43407
Cruise SFC	kg/daN/h	0.5399	0,5391	0,5382	0,5375	0,5365	0,5355	0,5354	0,5357	0,5364	0,5373	0,5384	0,5396
Cruise L/D	-	18.32	18,364	18,354	18,347	18,333	18,316	18,305	18,316	18,352	18,388	18,425	18,462
TOFL	m	1930	1934	1939	1944	1954	1973	1991	2000	2000	2000	2000	2000
App speed	kt	133,2	133	133,1	133,1	133,1	133,1	133,1	132,9	132,3	131,8	131,3	130,8
Vz TOC MCL rating	ft/min	470	469	469	470	471	474	477	479	482	485	487	490
Time to climb	min	25	25	25	25	25	25	25	25	25	25	25	25
Block fuel	kg	3701	3682	3679	3678	3681	3695	3715	3738	3764	3792	3822	3853
COC	$/trip	9892	9877	9875	9875	9878	9891	9909	9931	9956	9982	10010	10040
CO_2metric	10e-4kg /km/$m^{0.48}$	7774	7727	7719	7717	7721	7752	7796	7851	7915	7984	8057	8134

Table 6 Effect of e-fan power with electric chain efficiency at 95% - (b)

e-fan power	MW	-	0.05	0.15	0,25	0,5	1,0	1,5	2,0	2,5	3,0	3,5	4,0
e-chain mass	kg	-	31	93	154	308	617	925	1233	1542	1850	2158	2467
Effective ref thrust	daN	11460	11400	11377	11359	11322	11273	11235	11245	11238	11250	11265	11284
Turbofan nacelle mass	kg	7500	7458	7425	7396	7329	7212	7103	7017	6925	6842	6762	6685
Propulsion mass	kg	7500	7489	7518	7550	7637	7829	8028	8250	8467	8692	8920	9152
Wing area	m²	151,9	152	151,9	151,9	151,9	152,4	152,8	155,5	157,1	159,4	161,8	164,2
MTOW	kg	76840	76659	76658	76677	76754	77025	77337	77881	78340	78886	79448	80025
MLW	kg	67700	67609	67633	67668	67765	68040	68328	68852	69269	69768	70277	70793
OWE	kg	45270	45186	45209	45242	45332	45589	45858	46348	46737	47204	47679	48162
MWE	kg	40300	40222	40245	40278	40368	40625	40894	41384	41773	42240	42715	43198
Cruise SFC	kg/daN/h	0.5399	0,539	0,5378	0,5369	0,5352	0,533	0,5316	0,5307	0,5301	0,5298	0,5297	0,5298
Cruise L/D	-	18.32	18,363	18,352	18,343	18,323	18,302	18,283	18,329	18,343	18,378	18,414	18,450
TOFL	m	1930	1934	1940	1945	1957	1977	1997	1992	2000	2000	2000	2000
App speed	kt	133,2	133	133,1	133,1	133,3	133,3	133,4	132,7	132,5	132	131,5	131
Vz TOC MCL rating	ft/min	470	469	469	470	471	474	476	479	482	484	487	489
Time to climb	min	25	25	25	25	25	25	25	25	25	25	25	25
Block fuel	kg	3701	3681	3676	3673	3671	3675	3684	3697	3713	3731	3751	3772
COC	$/trip	9892	9877	9875	9875	9878	9891	9909	9931	9956	9982	10010	10040
CO_2metric	10e-4kg /km/$m^{0.48}$	7774	7727	7719	7717	7721	7752	7796	7851	7915	7984	8057	8134

Table 7 Effect of e-fan power with electric chain efficiency at 95% - (c)

e-fan power	MW	-	0.05	0.15	0,25	0,5	1,0	1,5	2,0	2,5	3,0	3,5	4,0
e-chain mass	kg	-	15	46	77	154	308	463	617	771	925	1079	1233
Effective ref thrust	daN	11460	11397	11368	11344	11293	11212	11144	11083	11049	11022	10998	10978
Turbofan nacelle mass	kg	7500	7457	7421	7390	7317	7185	7063	6946	6842	6743	6646	6551
Propulsion mass	kg	7500	7489	7518	7550	7637	7829	8028	8250	8467	8692	8920	9152
Wing area	m²	151,9	152	151,8	151,7	151,6	151,7	151,8	152	153,4	155	156,6	158,3
MTOW	kg	76840	76632	76573	76536	76484	76461	76493	76559	76752	76975	77214	77467
MLW	kg	67700	67586	67560	67546	67534	67552	67599	67664	67854	68067	68288	68517
OWE	kg	45270	45164	45141	45127	45116	45132	45176	45237	45415	45614	45821	46034
MWE	kg	40300	40200	40177	40163	40152	40168	40212	40273	40451	40650	40857	41070
Cruise SFC	kg/daN/h	0.5399	0,539	0,5378	0,5369	0,5352	0,5329	0,5315	0,5305	0,5299	0,5296	0,5295	0,5295
Cruise L/D	-	18.32	18,362	18,350	18,339	18,318	18,285	18,259	18,237	18,249	18,266	18,285	18,305
TOFL	m	1930	1934	1938	1943	1952	1968	1984	1998	2000	2000	2000	2000
App speed	kt	133,2	133	133,1	133,1	133,1	133,1	133,1	133,1	132,7	132,2	131,7	131,3
Vz TOC MCL rating	ft/min	470	469	469	469	471	473	475	477	479	481	483	485
Time to climb	min	25	25	25	25	25	25	25	25	25	25	25	25
Block fuel	kg	3701	3679	3672	3667	3659	3651	3649	3650	3654	3660	3668	3677
COC	$/trip	9892	9875	9869	9865	9859	9853	9852	9854	9859	9866	9874	9884
CO_2metric	10e-4kg /km/$m^{0.48}$	7774	7722	7705	7693	7674	7656	7652	7657	7672	7691	7715	7743

List of airplane descriptive variables in MARILib

Longitudinal positions are taken from nose cone.
Orders of magnitude are given as powers of ten.
The units presented are usual units.

Name	Unit	Order of magnitude	Description
design_driver			
design_range	NM	3	Range of design mission
cruise_mach	mach	-1	Nominal cruise Mach number
ref_cruise_altp	ft	4	Reference cruise altitude (generally 35000ft)
top_of_climb_altp	ft	4	Top of climb altitude (may be lower or equal to reference cruise altitude)

Name	Unit	Order of magnitude	Description
low_speed			
disa_tofl	degK	1	Temperature shift for take off field length computation
altp_tofl	ft	4	Altitude for take off field length computation
kvs1g_tofl	no_dim	0	Minimum allowed stall speed margin at take off
req_tofl	m	3	Maximum take off field length at MTOW and given conditions
eff_tofl	m	3	Effective take off field length at MTOW and given condition
eff_kvs1g	no_dim	0	Effective stall speed margin at take off
seg2_path	no_dim	0	Air path at 35 ft at take off
limitation	int	0	Active limitation
disa_app_speed	degK	1	Temperature shift for approach speed computation
altp_app_speed	ft	3	Altitude for approach speed computation
kvs1g_app_speed	no_dim	0	Minimum allowed stall speed margin at landing
req_app_speed	kt	2	Maximum approach speed at MLW and given conditions
eff_app_speed	kt	2	Effective approach speed at MLW and given condition
disa_oei	degK	1	Temperature shift for One Engine Inoperative (OEI)
req_oei_altp	ft	4	Required One Engine Inoperative (OEI) minimum altitude
req_oei_path	%	0	Required minimum slope OEI at 95%MTOW, required altitude and MCN rating
eff_oei_path	%	0	Effective slope OEI at 95%MTOW, required altitude and MCN rating
oei_best_speed	kt	2	Calibrated Air Speed (CAS) at which slope is maximum in given conditions

Name	Unit	Order of magnitude	Description
high_speed			
disa_climb	degK	1	Temperature shift for Maximum climb speed computation
req_vz_climb	ft/min	2	Required minimum climb speed at 97%MTOW, nominal initial cruise altitude and MCL rating
eff_vz_climb	ft/min	2	Effective climb speed at 97%MTOW, nominal initial cruise altitude and MCL rating
req_vz_cruise	ft/min	2	Required minimum climb speed at 97%MTOW, nominal initial cruise altitude and MCR rating
eff_vz_cruise	ft/min	2	Effective climb speed at 97%MTOW, nominal initial cruise altitude and MCR rating
req_toc_altp	ft	4	Targeted Top Of Climb Altitude (TOC) for Time To Climb (TTC) computation
cas1_ttc	kt	2	Calibrated Air Speed (CAS) below 10000ft for TTC computation
cas2_ttc	kt	2	Calibrated Air Speed (CAS) above 10000ft for TTC computation
req_ttc	min	1	Required maximum Time To Climb
eff_ttc	min	1	Effective Time To Climb
cruise_sfc	kg/daN/h	0	Specific fuel consumption in cruise
cruise_lod	no_dim	1	Lift over drag ratio in cruise

Name	Unit	Order of magnitude	Description
max_payload_mission			
range	NM	3	Range of the max payload mission
payload	kg	4	Payload of the max payload mission
tow	kg	4	Take off weight of the max payload mission
total_fuel	kg	4	Total fuel of the max payload mission
block_fuel	kg	4	Block fuel of the max payload mission
block_time	h	1	Block time of the max payload mission

Name	Unit	Order of magnitude	Description
nominal_mission			
range	NM	3	Range of the nominal mission
payload	kg	4	Payload of the nominal mission
tow	kg	4	Take off weight of the nominal mission
total_fuel	kg	4	Total fuel of the nominal mission
block_fuel	kg	4	Block fuel of the nominal mission
block_time	h	1	Block time of the nominal mission

Name	Unit	Order of magnitude	Description
max_fuel_mission			
range	NM	3	Range of the max fuel mission
payload	kg	4	Payload of the max fuel mission
tow	kg	4	Take off weight of the max fuel mission
total_fuel	kg	4	Total fuel of the max fuel mission
block_fuel	kg	4	Block fuel of the max fuel mission
block_time	h	1	Block time of the max fuel mission

Name	Unit	Order of magnitude	Description
zero_payload_mission			
range	NM	3	Range of the zero payload mission
tow	kg	4	Take off weight of the zero payload mission
total_fuel	kg	4	Total fuel of the zero payload mission
block_fuel	kg	4	Block fuel of the zero payload mission
block_time	h	1	Block time of the zero payload mission

Name	Unit	Order of magnitude	Description
cost_mission			
disa	degK	1	Temperature shift for cost evaluation mission computation
range	NM	3	Range of cost evaluation mission
payload	kg	4	Payload of the max cost mission
tow	kg	4	Take off weight of the max cost mission
total_fuel	kg	4	Total fuel of the max cost mission
block_fuel	kg	4	Block fuel of the max cost mission
block_time	h	1	Block time of the max cost mission
block_CO2	kg	4	Mass of carbon dioxide emitted during the mission

Name	Unit	Order of magnitude	Description
economics			
gear_price	M$	1	Price of landing gears
engine_price	M$	1	Price of one engine
battery_price	$/kg	1	Mass price of battery (if any)
airplane_price	M$	1	Price of the airplane
fuel_price	$/gal	1	Fuel price
labor_cost	$/h	1	Labor cost
irp	year	1	Interest recovery period
period	year	1	Utilisation period
interest_rate	%	1	Interest rate
utilisation	int	3	Number of flights per year
cockpit_crew_cost	$/trip	3	Cockpit crew cost
cabin_crew_cost	$/trip	3	Cabin crew cost
fuel_cost	$/trip	3	Fuel cost
landing_fees	$/trip	3	Landing fees
navigation_fees	$/trip	3	Navigation fees
catering_cost	$/trip	3	Catering cost
pax_handling_cost	$/trip	3	Pax handling cost
ramp_handling_cost	$/trip	3	Ramp handling cost
standard_operating_cost	$/trip	4	Standard operating cost
cash_operating_cast	$/trip	4	Cash operating cost
total_investment	$/trip	6	Total investment
insurance	$/trip	6	Inssurance
depreciation	$/trip	5	Depreciation
direct_operating_cost	$/trip	6	Direct operating cost

Name	Unit	Order of magnitude	Description
environmental_impact			
rgf	m^2	2	Reference Geometric Factor, close to the cabin floor pressurized area
CO2_metric	kg/km/$m^{0.48}$	-4	Fuel efficiency metric
CO2_index	g/kg	3	Mass of carbon dioxid emited per kilogram of fuel
H2O_index	g/kg	3	Mass of water emitted per kilogram of fuel
SO2_index	g/kg	0	Mass of sulfur dioxid emitted per kilogram of fuel
NOx_index	g/kg	0	Mass of nitrogen dioxid emitted per kilogram of fuel
CO_index	g/kg	0	Mass of carbon monoxid emitted per kilogram of fuel
HC_index	g/kg	0	Mass of unburnt hydrocarbon emitted per kilogram of fuel
Sulfuric_acid_index	g/kg	0	Mass of sulfuric acid emitted per kilogram of fuel
nitrous_acid_index	g/kg	0	Mass of nitrous acid emitted per kilogram of fuel
nitric_acid_index	g/kg	0	Mass of nitric acid emitted per kilogram of fuel
soot_index	int	12	Number of soot particle emitted per kilogram of fuel

Name	Unit	Order of magnitude	Description
aerodynamics			
cruise_lod_max	no_dim	1	Maximum lift over drag ratio in cruise
cz_cruise_lod_max	no_dim	0	Lift coefficient corresponding to maximum lift over drag
hld_conf_clean	no_dim	0	High lift device setting in clean configuration (0 by definition)
cz_max_clean	no_dim	0	Maximum lift coefficient in clean wing configuration
hld_conf_to	no_dim	0	High lift device setting in take off configuration (0 < hld_conf < 0.6)
cz_max_to	no_dim	0	Maximum lift coefficient in take off configuration
hld_conf_ld	no_dim	0	High lift device setting in landing configuration (nominal value is 1)
cz_max_ld	no_dim	0	Maximum lift coefficient in landing configuration

Name	Unit	Order of magnitude	Description
propulsion			
architecture	int	0	Propulsion architecture, 1:turbofan, 2:partial turbo electric n°1
fuel_type	int	0	Type of fuel, 1:kerosene, 2:hydrogene
reference_thrust_effective	daN	5	Effective SLST computed as max thrust(Mach = 0.25, ISA+15, Sea Level) / 0.8
sfc_cruise_ref	kg/daN/h	0	Specific Fuel Consumption in cruise condition, isa, ref_cruise_altp, cruise_mach
sec_cruise_ref	kW/daN/h	0	Specific Energy Consumption of the electric chain in cruise condition, isa, ref_cruise_altp, cruise_mach
bli_effect	int	0	BLI effect switch, 0: without, 1: with
bli_e_thrust_factor	no_dim	0	Thrust factor at constant power due to boundary layer ingestion of the electric fan
bli_thrust_factor	no_dim	0	Thrust factor at constant power due to boundary layer ingestion of the turbofans
rating_code	int	0	Array of rating codes [0:MTO, 1:MCN, 2:MCL, 3:MCR, 4:FID]
mto_thrust_ref	daN	4	Turbofan thrust in take off rating (one engine), Sea Level, ISA+15, Mach 0.25
mcn_thrust_ref	daN	4	Turbofan thrust in maxi continuous rating (one engine), Required ceiling altitude, ISA, cruise Mach
mcl_thrust_ref	daN	4	Turbofan thrust in max climb rating (one engine), Required Top of Climb altitude, ISA, cruise Mach
mcr_thrust_ref	daN	4	Turbofan thrust in max cruise rating (one engine), Reference cruise altitude, ISA, cruise Mach
fid_thrust_ref	daN	4	Turbofan thrust in flight idle rating (one engine), Reference cruise altitude, ISA, cruise Mach
mass	kg	4	Total mass of the propulsion system (pylons, nacelles, engines, ...)
c_g	m	1	Global CG position for thr whole propulsion system (pylons, nacelles, engines, ...)

Name	Unit	Order of magnitude	Description
weights			
mwe	kg	4	Manufacturer Weight Empty
owe	kg	4	Operating Weight Empty (= mwe + m_op_item + m_cont_pallet)
mzfw	kg	4	Maximum Zero Fuel Weight (= owe + n_pax_ref.m_pax_max)
mlw	kg	4	Maximum Landing Weight (close or equal to 1.07 mzfw except for small aircraft where mlw = mtow)
mtow	kg	4	Maximum Take Off Weight
mfw	kg	4	Maximum Fuel Weight

Name	Unit	Order of magnitude	Description
center_of_gravity			
mwe	m	1	Longitudinal position of MWE CG
owe	m	1	Longitudinal position of OWE CG
max_fwd_mass	kg	2	Aircraft mass at maximum forward CG
max_fwd_req_cg	m	1	Required maximum forward CG
max_fwd_trim_cg	m	1	Maximum trimmable forward CG
max_bwd_mass	kg	2	Aircraft mass at maximum backward CG
max_bwd_req_cg	m	1	Required maximum backward CG
max_bwd_stab_cg	m	1	Maximum backward CG

Name	Unit	Order of magnitude	Description
cabin			
n_pax_ref	int	2	Reference Number of passengers (most often 2 class layout)
n_aisle	int	0	Number of aisle in economic section
n_pax_front	int	0	Number of seats in a row in economic section
fwd_limit	m	0	Distance between aircraft nose and cabin forward limit
width	m	0	Maximum width of the cabin (not floor width)
length	m	1	Total length of the cabin
floor_area	m^2	2	Area of the cabin taking into account its maximum width (not real floor area)
m_furnishing	kg	3	Total mass of furnishing equipements
m_op_item	kg	3	Total mass of operator items
cg_furnishing	kg	3	Center of gravity of furnishing equipements
cg_op_item	kg	3	Center of gravity of operator items

Name	Unit	Order of magnitude	Description
payload			
m_pax_nominal	kg	2	Mass allowance per passenger to compute nominal payload
m_pax_max	kg	2	Mass allowance per passenger to compute maximum payload
m_container_pallet	kg	3	Mass of containers or pallets empty
nominal	kg	4	Mass of nominal payload
maximum	kg	4	Mass of maximum payload
max_fwd_mass	kg	2	Payload mass at maximum forward payload CG
max_fwd_req_cg	m	1	Required maximum forward CG
max_bwd_mass	kg	2	Payload mass at maximum backward payload CG
max_bwd_req_cg	m	1	Required maximum backward CG
cg_container_palet	m	1	Center of gravity of containers or pallets empty

Name	Unit	Order of magnitude	Description
fuselage			
width	m	0	Fuselage width of the cylindrical part
height	m	0	Fuselage height of the cylindrical part
length	m	1	Total fuselage length
tail_cone_length	m	0	Length of rear evolutive part of the fuselage
net_wetted_area	m^2	2	Fuselage total net wetted area
mass	kg	3	Equiped fuselage mass (without systems)
c_g	m	1	Longitudinal position of the fuselage CG

Name	Unit	Order of magnitude	Description
wing			
attachment	int	0	Wing attachment, 1: low wing, 2: high wing
morphing	int	0	Wing deformation driver, 1-> aspect ratio, 2-> span
hld_type	int	0	Type of high lift devices
t_o_c_r	%	1	Thickness over chord ratio of the wing at root
t_o_c_k	%	1	Thickness over choerd ratio of the wing at main kink
t_o_c_t	%	1	Thickness over chord ratio at wing tip
sweep	deg	0	Wing sweep angle at 25% of the chord
dihedral	deg	0	Mean dihedral of the wing
setting	deg	0	Setting angle of the wing at root
taper_ratio	no_dim	0	Wing taper ratio
aspect_ratio	no_dim	0	Wing aspect ratio
area	m^2	2	Wing reference area (planform)
span	m	1	Wing span
mac	m	0	Mean aerodynamic chord of the wing
net_wetted_area	m^2	2	Wing total net wetted area
mass	kg	3	Equiped wing mass (without systems)
c_g	m	1	Longitudinal position of the wing CG
x_root	m	1	Longitudinal position of 0% of wing root chord
y_root	m	0	Span wise position of 0% of the wing root chord
z_root	m	0	Vertical position of 0% of the wing root chord
c_root	m	0	Wing root chord length
x_kink	m	1	Longitudinal position of 0% of wing kink chord
y_kink	m	0	Span wise position of 0% of the wing kink chord
z_kink	m	0	Vertical position of 0% of the wing kink chord
c_kink	m	0	Wing kink chord length
x_tip	m	1	Longitudinal position of 0% of wing tip chord
y_tip	m	0	Span wise position of 0% of the wing tip chord
z_tip	m	0	Vertical position of 0% of the wing tip chord
c_tip	m	0	Wing tip chord length
x_mac	m	1	Longitudinal position of wing mean aerodynamic chord
y_mac	m	0	Span wise position of wing mean aerodynamic chord

Name	Unit	Order of magni-tude	Description
landing_gears			
mass	kg	3	Mass of landing gears (nose and main)
c_g	m	1	Longitudinal position of the landing gears CG

Name	Unit	Order of magnitude	Description
horizontal_tail			
attachment	int	0	Type of horizontal tail, 1: classical, 2: T-tail
sweep	deg	0	Horizontal tail sweep angle at 25% of th echords
taper_ratio	no_dim	0	Taper ratio of the horizontal tail
aspect_ratio	no_dim	0	Aspect ratio of the horizontal tail
dihedral	deg	0	Mean dihedral of the horizontal tail
volume	no_dim	0	Volume coefficient of the horizontal tail
lever_arm	m	1	Lever arm of the horizontal tail (from 25% wing MAC to 25% HTP MAC)
area	m^2	2	Horizontal tail reference area
span	m	2	Horizontal tail span
mac	m	0	Mean aerodynamic part of the horizontal tail
net_wetted_area	m^2	2	Total net wetted area of the horizontal tail
mass	kg	2	Equiped mass of the horizontal tail
c_g	m	1	Longitudinal position of the CG of the horizontal tail
x_axe	m	2	Longituidinal position of the horizontal tail central chord
z_axe	m	1	Vertical position of the horizontal tail central chord
c_axe	m	1	Horizontal tail central chord
x_tip	m	2	Longitudinal position of the horizontal tail tip chord
y_tip	m	1	Lateral position of the horizontal tail tip chord
z_tip	m	1	Vertical position of the horizontal tail tip chord
c_tip	m	1	Horizontal tail tip chord
x_mac	m	2	Longitudinal position of the horizontal tail mean aerodynamic chord
y_mac	m	1	Lateral position of the horizontal tail mean chord

Name	Unit	Order of magni-tude	Description
vertical_tail			
sweep	deg	0	Vertical tail sweep angle at 25% of th echords
taper_ratio	no_dim	0	Taper ratio of the vertical tail
aspect_ratio	no_dim	0	Aspect ratio of the vertical tail
t_o_c	no_dim	0	Thickness to chord ratio of the vertical tail
dihedral	deg	0	Mean dihedral of the vertical tail
volume	m^2/kN	0	Volume coefficient of the vertical tail
lever_arm	m	1	Lever arm of the vertical tail (from 25% wing MAC to 25% HTP MAC)
area	m^2	2	Vertical tail reference area
height	m	1	Height of the vertical tail
mac	m	0	Mean aerodynamic part of the vertical tail
net_wetted_area	m^2	2	Total net wetted area of the vertical tail
mass	kg	2	Equiped mass of the vertical tail
c_g	m	1	Longitudinal position of the CG of the vertical tail
x_root	m	2	Longituidinal position of the vertical tail root chord
z_root	m	1	Vertical position of the vertical tail root chord
c_root	m	1	Vertical tail root chord
x_tip	m	2	Longitudinal position of the vertical tail tip chord
z_tip	m	1	Vertical position of the vertical tail tip chord
c_tip	m	1	Vertical tail tip chord
x_mac	m	2	Longitudinal position of the vertical tail mean aerodynamic chord

Name	Unit	Order of magni-tude	Description
tanks			
cantilever_volume	m^3	1	Volume of tanks in the cantilever wing
central_volume	m^3	1	Volume of tanks in the central part of the wing (inside the fuselage)
mfw_volume_limited	m^3	1	Maximum geometrical fuel volume
fuel_density	kg/m^3	2	Fuel density
fuel_cantilever_cg	m	1	Center of gravity of tanks in the cantilever wing
fuel_central_cg	m	1	Center of gravity of tanks in the central part of the wing (inside the fuselage)
fuel_body_cg	m	1	Center of gravity of tanks in the nacelle bodies
fuel_max_fwd_mass	kg	3	Fuel mass of max forward fuel cg
fuel_max_fwd_cg	m	1	Max forward fuel cg
fuel_max_bwd_mass	kg	3	Fuel mass of max backward fuel cg
fuel_max_bwd_cg	m	1	Max backward fuel cg

Name	Unit	Order of magni-tude	Description
systems			
mass	kg	3	Mass of all airplane systems
c_g	m	1	Longitudinal position of the system CG

Name	Unit	Order of magni-tude	Description
turbofan_pylon			
mass	kg	3	Equiped mass of the pylons
c_g	m	1	Longitudinal position of the CG of the pylons

Name	Unit	Order of magni-tude	Description
turbofan_nacelle			
attachment	int	0	Nacelle attachment (1= under wing, 2= rear fuselage)
width	m	0	Maximum width of the nacelles
length	m	0	Length of the fan cowl
x_ext	m	1	Longitudinal position of the center of the air inlet of the external engine
y_ext	m	1	Span wise position of the center of the air inlet of the external engine
z_ext	m	0	Vertical position of the center of the air inlet of the external engine
x_int	m	1	Longitudinal position of the center of the air inlet of the internal engine
y_int	m	1	Span wise position of the center of the air inlet of the internal engine
z_int	m	0	Vertical position of the center of the air inlet of the internal engine
net_wetted_area	m^2	1	Total net wetted area of the nacelles (fan cowls)
efficiency_fan	no_dim	0	Fan efficiency for turbofan (capability to turn shaft power into kinetic energy)
efficiency_prop	no_dim	0	"Propeller like" Fan+Cowl efficiency for turbofan
hub_width	m	0	Diameter of the hub of the fan (for pusher fan only)
fan_width	m	0	Diameter of the fan of the turbofan nacelle
nozzle_width	m	0	Diameter of the nozzle of the turbofan nacelle
nozzle_area	m^2	0	Exhaust nozzle area of the turbofan nacelle
body_length	m	0	Length of the body in front of the turbofan nacelle
bnd_layer	m	0	Boundary layer thickness law in front of the fan
mass	kg	3	Equiped mass of the nacelles (including engine masses)
c_g	m	1	Longitudinal position of the CG of the nacelles

Name	Unit	Order of magnitude	Description
turbofan_engine			
n_engine	int	0	Number of turbofans
bpr	no_dim	0	By Pass Ratio of the turbofans
reference_thrust	daN	4	Design Reference thrust of the turbofan
rating_factor	no_dim	0	Array of rating factors versus maximum thrust
core_thrust_ratio	no_dim	0	Fraction of the total thrust of a turbofan which is due to the core (typically between 10% and 16% for BPR>5)
core_width_ratio	no_dim	0	Fraction of the total nacelle diameter which is taken by the core
core_weight_ratio	no_dim	0	Fraction of the total nacelle mass which is taken by the core
kfn_off_take	no_dim	0	SLST thrust factor due to power off take (if any)

Name	Unit	Order of magnitude	Description
turboprop_pylon			
mass	kg	3	Equiped mass of the pylons
c_g	m	1	Longitudinal position of the CG of the pylons

Name	Unit	Order of magnitude	Description
turboprop_nacelle			
width	m	0	Maximum width of the nacelle
length	m	0	Length of the nacelle
x_ext	m	1	Longitudinal position of the center of the propeller
y_ext	m	1	Span wise position of the center of the propeller
z_ext	m	0	Vertical position of the center of the propeller
net_wetted_area	m^2	1	Total net wetted area of the nacelles
mass	kg	3	Equiped mass of the nacelles (including engine masses)
c_g	m	1	Longitudinal position of the CG of the nacelles

Name	Unit	Order of magnitude	Description
turboprop_engine			
n_engine	int	0	Number of turbofans
reference_thrust	daN	4	Design Reference thrust of the turboprop
reference_power	shp	4	Reference power of the turboprop
rating_factor	no_dim	0	Array of rating factors versus maximum thrust
propeller_diameter	no_dim	0	Diameter of the propeller
propeller_efficiency	no_dim	0	Efficiency of the propeller in cruise condition

Name	Unit	Order of magnitude	Description
body_nacelle			
width	m	0	Maximum width of the nacelle body
length	m	0	Length of the nacelle body
x_axe	m	1	Longitudinal position of the center of the nacelle body nose
y_axe	m	1	Span wise position of the center of the nacelle body nose
z_axe	m	0	Vertical position of the center of the nacelle body nose
net_wetted_area	m^2	1	Total net wetted area of the nacelle bodies
mass	kg	3	Equiped mass of the nacelle bodies without engines
c_g	m	1	Longitudinal position of the CG of the nacelle body

Name	Unit	Order of magnitude	Description
power_elec_chain			
mto	uc	0	Tale off power, mto<1: turbofan shat power ratio off take, mto>1: e-fan motor power
mcn	uc	0	Maxi continuous power, mcn<1: turbofan shat power ratio off take, mcn>1: e-fan motor power
mcl	uc	0	Max climb power, mcl<1: turbofan shat power ratio off take, mcl>1: e-fan motor power
mcr	uc	0	Max cruise power, mcr<1: turbofan shat power ratio off take, mcr>1: e-fan motor power
fid	uc	0	Flight idle power, fid<1: turbofan shat power ratio off take, fid>1: e-fan motor power
max_power	kW	4	E-fan motor maximum power
max_power_rating	int	0	Engine rating of e-fan motor maximum power
overall_efficiency	no_dim	0	Power efficiency of the electric chain
generator_pw_density	kW/kg	0	Power density of electric generation
rectifier_pw_density	kW/kg	0	Power density of rectifiers
wiring_pw_density	kW/kg	0	Power density of wiring
cooling_pw_density	kW/kg	0	Power density of cooling system
mass	kg	2	Mass of the electric chain (generator, rectifier, wires, cooling)
c_g	m	1	Longitudinal position of the CG of the electric chain

Name	Unit	Order of magni-tude	Description
electric_nacelle			
width	m	0	Maximum width of the electric fan cowl
length	m	0	Length of the electric fan cowl
x_axe	m	1	Longitudinal position of the center of the electric nacelle air inlet
y_axe	m	1	Span wise position of the center of the electric nacelle air inlet
z_axe	m	0	Vertical position of the center of the electric nacelle air inlet
net_wetted_area	m^2	1	Total net wetted area of the electric fan nacelle (fan cowl)
efficiency_fan	no_dim	0	Fan efficiency for electric fan (capability to turn shaft power into kinetic energy)
efficiency_prop	no_dim	0	”Propeller like” Fan+Cowl efficiency for electric fan
motor_efficiency	no_dim	0	Motor efficiency
motor_pw_density	kW/kg	0	Power density of electric motor
controler_efficiency	no_dim	0	Controler electric efficiency
controler_pw_density	kW/kg	0	Power density of controlers
nacelle_pw_density	kW/kg	0	Power density of efan nacelle and mountings
hub_width	m	0	Diameter of the hub of the electric fan (for pusher fan only)
fan_width	m	0	Diameter of the electric fan
nozzle_width	m	0	Diameter of the nozzle of theelectric nacelle
nozzle_area	m^2	0	Exhaust nozzle area of the electric nacelle
body_length	m	0	Length of the body in front of the electric nacelle
bnd_layer	structure	0	Boundary layer thickness law in front of the e-fan 2darray
mass	kg	2	Equiped mass of the nacelle of the electric fan (including the controler, motor and nacelle)
c_g	m	1	Longitudinal position of the CG of the electric nacelle

Name	Unit	Order of magnitude	Description
electric_engine			
mto_e_power_ratio	no_dim	0	Turbofan off take power ratio in take off rating (one engine), Sea Level, ISA+15, Mach 0.25
mto_e_shaft_power	kW	3	E-fan shaft power in take off rating (one engine), Sea Level, ISA+15, Mach 0.25
mto_e_fan_thrust	daN	3	E-fan thrust in take off rating (one engine), Sea Level, ISA+15, Mach 0.25
mcn_e_power_ratio	no_dim	0	Turbofan off take power ratio maxi continuous rating (one engine), Required ceiling altitude, ISA, cruise Mach
mcn_e_shaft_power	kW	3	E-fan shaft power in maxi continuous rating (one engine), Required ceiling altitude, ISA, cruise Mach
mcn_e_fan_thrust	daN	3	E-fan thrust in maxi continuous rating (one engine), Required ceiling altitude, ISA, cruise Mach
mcl_e_power_ratio	no_dim	0	Turbofan off take power ratio in max climb rating (one engine), Required Top of Climb altitude, ISA, cruise Mach
mcl_e_shaft_power	kW	3	E-fan shaft power in max climb rating (one engine), Required Top of Climb altitude, ISA, cruise Mach
mcl_e_fan_thrust	daN	3	E-fan thrust in max climb rating (one engine), Required Top of Climb altitude, ISA, cruise Mach
mcr_e_power_ratio	no_dim	0	Turbofan off take power ratio in max cruise rating (one engine), Reference cruise altitude, ISA, cruise Mach
mcr_e_shaft_power	kW	3	E-fan shaft power in max cruise rating (one engine), Reference cruise altitude, ISA, cruise Mach
mcr_e_fan_thrust	daN	3	E-fan thrust in max cruise rating (one engine), Reference cruise altitude, ISA, cruise Mach
fid_e_power_ratio	no_dim	0	Turbofan off take power ratio in flight idle rating (one engine), Reference cruise altitude, ISA, cruise Mach
fid_e_shaft_power	kW	3	E-fan shaft power in flight idle rating (one engine), Reference cruise altitude, ISA, cruise Mach
fid_e_fan_thrust	daN	3	E-fan thrust in flight idle rating (one engine), Reference cruise altitude, ISA, cruise Mach
flight_data	structure	dict	Dictionary of flying conditions for each rating "disa":array, "altp":array, "mach":array, "nei":array

Name	Unit	Order of magnitude	Description
battery			
strategy	int	0	Battery sizing strategy, 1: power_feed and energy_cruise driven, 2: battery mass driven
power_feed	kW	4	Power delivered to e-fan(s) at take off and(or) climb during a total of time_feed
time_feed	min	1	Maximum duration of the power_feed delivered to e-fan(s)
energy_cruise	kWh	1	Total battery energy dedicated to cruise
energy_density	kWh/kg	0	Battery energy density
power_density	kW/kg	0	Battery power density (capability to release power per mass unit
mass	kg	3	Total battery mass
c_g	m	1	Global CG of batteries

Acknowledgments

The authors wish to thank Serge Bonnet, Airbus Senior Expert in Overall Aircraft Design for his review and advise as weel as the Institute of Technology IRT Saint-Exupéry researchers for their valuable support.

References

[1] Gould, N. I., Orban, D., and Toint, P. L., "CUTEr and SifDec: A constrained and unconstrained testing environment, revisited," *ACM Transactions on Mathematical Software (TOMS)*, Vol. 29, No. 4, 2003, pp. 373–394.

[2] Gould, N. I., Orban, D., and Toint, P. L., "CUTEst: a constrained and unconstrained testing environment with safe threads for mathematical optimization," *Computational Optimization and Applications*, Vol. 60, No. 3, 2015, pp. 545–557.

[3] Martins, J. R. R. A., and Lambe, A. B., "Multidisciplinary Design Optimization: A Survey of Architectures," *AIAA Journal*, Vol. 51, No. 9, 2013, pp. 2049–2075. doi:10.2514/1.J051895.

[4] Agte, J. S., Sobieszczanski-Sobieski, J., and Sandusky, R. R., "Supersonic business jet design through bi-level integrated system synthesis," Tech. rep., SAE Technical Paper, 1999.

[5] MacDonald, T., Clarke, M., Botero, E. M., Vegh, J. M., and Alonso, J. J., "SUAVE: an open-source environment enabling multi-fidelity vehicle optimization," *18th AIAA/ISSMO Multidisciplinary Analysis and Optimization Conference*, 2017, p. 4437.

[6] Kao, J., Hwang, J., Martins, J., Gray, J. S., and Moore, K. T., "A modular adjoint approach to aircraft mission analysis and optimization," *56th AIAA/ASCE/AHS/ASC Structures, Structural Dynamics, and Materials Conference*, 2015, p. 0136.

[7] Gallard, F., Vanaret, C., Guénot, D., Gachelin, V., Lafage, R., Pauwels, B., Barjhoux, P.-J., and Gazaix, A., "GEMS: A Python Library for Automation of Multidisciplinary Design Optimization Process Generation," *2018 AIAA/ASCE/AHS/ASC Structures, Structural Dynamics, and Materials Conference*, 2018, p. 0657.

[8] Gallard, F., Barjhoux, P., Olivanti, R., and A., G., "GEMS, a Generic Engine for MDO Scenarios : Key Features In Application," *2019 AIAA AVIATION Forum*, 2019.

[9] Raymer, D., *Aircraft Design: A Conceptual Approach 5e and RDSWin STUDENT*, American Institute of Aeronautics and Astronautics, Inc., 2012.

[10] Torenbeek, E., *Synthesis of subsonic airplane design: an introduction to the preliminary design of subsonic general aviation and transport aircraft, with emphasis on layout, aerodynamic design, propulsion and performance*, Springer Science & Business Media, 2013.

[11] Roskam, J., "Airplane Design Parts I to VIII," *nalysis Research Corporation*, 2002.

[12] Sforza, P. M., *Commercial airplane design principles*, Elsevier, 2014.

[13] Anderson, J. D., *Aircraft performance and design*, Vol. 1, WCB/McGraw-Hill Boston, MA, 1999.

[14] Shevell, R. S., and Shevell, R. S., *Fundamentals of flight*, Vol. 2, Prentice Hall Englewood Cliffs, NJ, 1989.

[15] Roux, E., "Pour une approche analytique de la dynamique du vol," *These, SUPAERO-ONERA*, 2005.

[16] Birman, J., "Uncertainty quantification and propagation in Conceptual Aircraft Design: from deterministic optimization to chance constrained optimization," Ph.D. thesis, Ph. D. thesis. University of Toulouse III-Paul Sabatier, 2013.

[17] Welstead, J., and Felder, J. L., "Conceptual design of a single-aisle turboelectric commercial transport with fuselage boundary layer ingestion," *54th AIAA Aerospace Sciences Meeting*, 2016, p. 1027.